Late Glacial to Early Holocene alluvial fans on the flanks of the Rhône valley (Central Valais, Switzerland)

Pierre Stalder

Abstract

After the demise of the Rhône glacier, Late Glacial to Early Holocene alluvial fans covered the Penninic substratum of the Rhône valley flanks (central Valais, Switzerland) and then were partly eroded before loess was deposited. Towards the end of the fans' building phase, as the local sources (rock glaciers and water expanses) became exhausted, the constitutive stacks of debris-flow, subordinate sand-flow (South flank only) and torrential deposits were capped by chaotic ones enriched in Rhône glacier and local moraine material as well as pieces of substratum. The emplacement of the voluminous S flank fans contributed to the filling of the valley and likely preceded that of the Sierre landslide. Although probable, this cannot be demonstrated on the opposite side. Testimony of the slopes' instability, significant land-sliding took place on the largest fan of the S flank. The sequence of events, which is common to both sides of the valley, is interpreted as a response to permafrost melting and abundant precipitations induced by regional warming. This story very much differs from the current one wherein Rhône glacier deposits cover the valley flanks.

Keywords Rhône valley . Rhône glacier. Geomorphology . Alluvial fans . Landslide . Debris-flow deposit . Sand-flow deposit . Chaotic deposit . Imbrication . Rock glacier .

Dedication This work is dedicated to late Prof. Marcel Burri who was a pioneer of Quaternary studies in Valais and gracefully agreed with large parts of this work.

1 Introduction

In the area of interest, the lower flanks of the central Rhône valley (RV, Fig.1) consist of Penninic substratum covered by Quaternary deposits currently interpreted as "Glaciaire rhodanien" (GR) by Badoux et al. (1959) or "Moraines de la dernière glaciation (MdG) by Gabus et al. (2008a and b). During a visit to relevant exposures, this interpretation was questioned whereby debris-, sand-flow and torrential deposits were preferred to moraines. To resolve this discrepancy, an area wide re-investigation of the Quaternary deposits was undertaken which results are reported below.

Throughout the area, the loess sets an approximate 10kb BP minimum age of the events described (Guélat 2013), which needs to be locally reassessed. It is understood as a brown silt layer of aeolian origin resting unconformably/disconformably on older deposits, generally less than a meter thick and consisting mainly of quartz with small amounts of feldspar, biotite, tourmaline, oxidized twig remains and/or their decomposition products.

Abbreviations

CH Chelin, CS Les Clous, CL Creta Limbo, DFD debris-flow deposit, FL Les Fleurs, OR Les Ormeaux, RG Rhône glacier, RR Réchy river, RV Rhône valley, SD slope deposit, SFD sans -flow deposit, SGA Swiss Geological Atlas, SL Sierre landslide, TL Top Layer, VAL Valençon, VR Réchy valley.

Pierre Stalder

p.j.stalder@bluewin.ch

2 Methodology

Conventional field geology (stratigraphy, structure, mapping, petrography), basic rock analysis (binocular lens and simple granulometry) and morphological analysis were the tools used. For lack of financial support, thin section analyses, quantitative analyses (X-ray) and age datings (OSL, $C_{14)}$ could not be carried out.
The grain size distribution was measured on dry samples using home-made square mesh sieves (6, 1.5, 0.6, 0.3 and 0.1 mm) with intervening steps of washing and drying. Maximum gravel clast size was set at 80 mm and sample size varied from 0.5 to 2.5 kg, depending on sorting and grain size. This method, which claims neither high precision nor accuracy, was deemed adequate for the stated objective.
The petrographic/mineralogical composition of the various grain-size fractions of representative samples was determined and summarized.

3 General morphological and geological settings

The RV cuts across a stack of alpine nappes, its axis coinciding with the trace of the Simplon-Rhône dextral transcurrent fault zone (Steck et al. 2001). Its flanks were shaped by the advances and retreats of the Rhône glacier (RG) and of its lateral branches (Burri 1955; Winistörfer 1978; Dorthe-Monachon 1993). During the Last Glacial Maximum, the RG surface reached about 2000 m in the area of interest (Bini et al. 2011). As argued below, the Quaternary cover of the lower flanks mostly consists of slope deposits (*SD)* and not of GR or MdG as shown on respectively sheets 35 and 111 of the Swiss geological Atlas (SGA).

Hills are emerging from the valley floor (Fig. 1) which are remnants of the Sierre landslide (SL) (Burri 1997; Schaechtelin 2000a and b; Gabus et al. lit. cit.). The timing of the latter's emplacement, its thickness and the underlying formations are poorly known. Based on gravimetry, the top of the substratum at the center of the RV lies some 500 m below the current surface (Rosselli and Olivier 2003). This figure is confirmed on seismic reflexion lines, one of which shows *SD* down to about 300 m a. m. s. l. on the N flank, some 6 km SW of the investigated area (Besson et al. 1993).

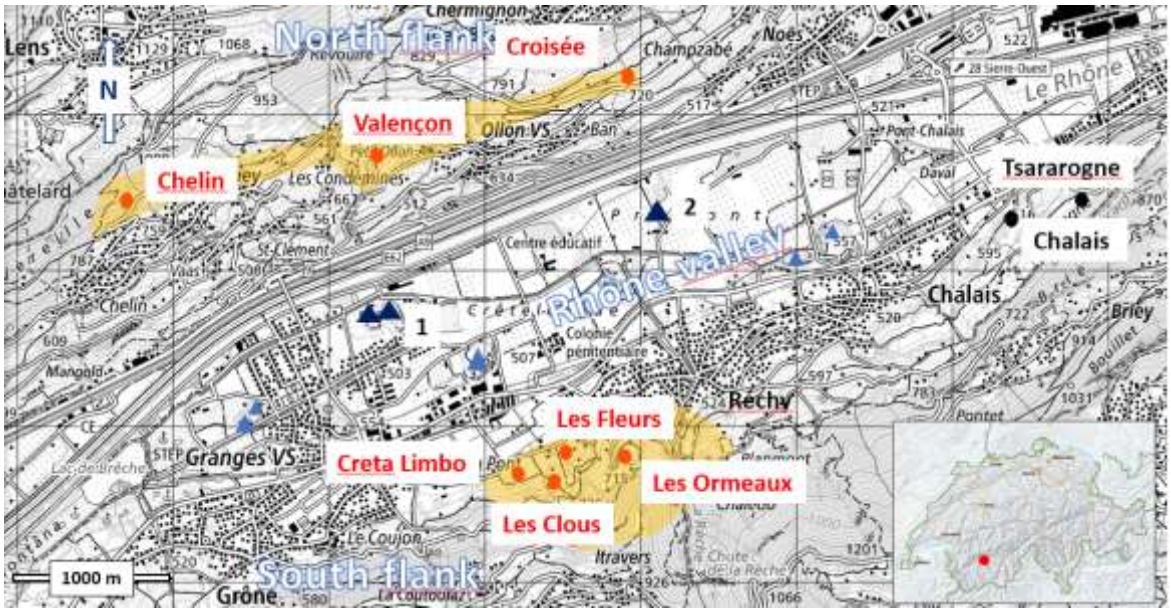

Fig. 1 Situation of the areas (yellow shade) and sites (red dots) investigated. Black dots refer to quarries mentioned in the text. Light blue triangles in the RV represent hills of the SL, the dark blue ones being topped by palaeo-Rhône alluvions. 2018 swisstopo base.

4 The North flank: Chelin, Valençon and Croisée

4.1 Geological framework

Below about 1200-1300 m the substratum of the Quaternary cover consists of the NNW dipping calcareous-sandy formations of the Lower Penninic Sion-Courmayeur zone (Badoux et al. lit. cit.; Gabus et al. lit. cit.). The structurally underlying calcareous-shaly Jurassic formations of the Helvetic Wildhorn nappe exposed at higher altitude provided most of the *SD* material which also included components of RG moraine and kame terrace scattered on the slopes.

From the RV floor to about 1500 m, the Quaternary cover is labelled GR on SGA sheet 35 and MdG to about 2500 m on adjacent sheet 111. However, the spectacular Chelin (CH) and Valençon (VAL) and the modest Croisée exposures tell a very different story (Figs 1 and 2).

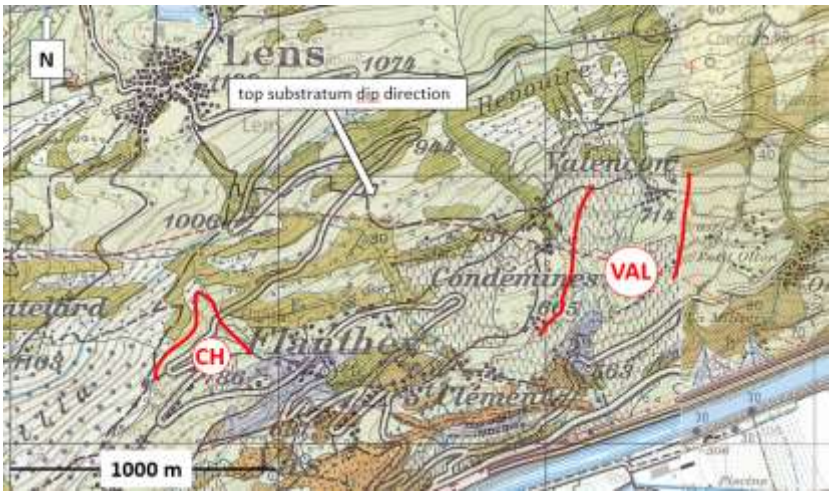

Fig. 2 Excerpt of SGA sheets 35 and 111 showing the current extensions of the CH and VAL bodies (inside the red lines). The light green colour covers undifferentiated RG and MdG deposits, the olive the Penninic substratum, the violet and orange the older formations

4.2 Morphology

The VAL topographical bulge and ravine are the prominent features of a generally smooth N flank partly covered by vineyards and dissected by gullies exposing the substratum and its cover (Fig. 2). The development of this rather subdued morphology started with the carving of the flank by the RG, continued with the emplacement of *SD* and their partial erosion, and ended with the deposition of the loess and subsequent erosion.

4.3 Chelin

There, Burri (1958) mentions stratified moraine consisting of counter-slope dipping layers. Stratification indeed there is, but layers dip down-slope as shown on a 20 m high cliff (UTM coord. 2’600’740/1’124’440) and in the neighbourhood. In addition, the former clearly unveils a complex stratigraphy that is unexpected in moraine environment (Figs 3 and 4). The layers of the substratum exposed in the vicinity dip at 30° towards SE and their eroded surface at 21° in the same direction.

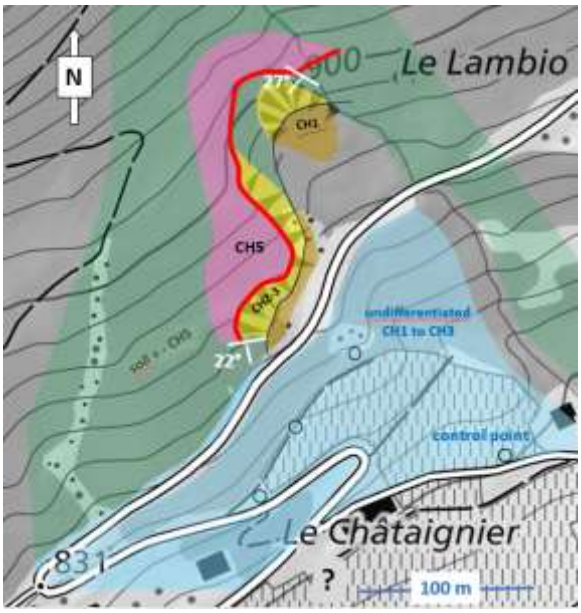

Fig. 3 Geological map of CH and immediate surroundings. The red line represents the thin CH4 unit. Circles are control points. 1918 swisstopo base.

4.3.1 General description and structure

The CH bulging body of *SD* is bound by unconformities at its contacts with the substratum and the loess (Figs 4 and 5). Bottom upwards, it is comprised of

- the **CH1, CH2** and **CH3** units of mud-supported gravel beds interpreted as stacks of debris-flow deposits (*DFD as* discussed in Chap. 4.6) and separated by a "pseudo-onlap" of CH2 on the CH1b conglomerate and by a colour change at the CH3-CH2 contact;
- the chaotic **CH4** unit unconformably overlying CH3.

The CH5a **loess,** which rests unconformably over the CH4 or older units, is conformably overlain by the CH5b gravel bed.

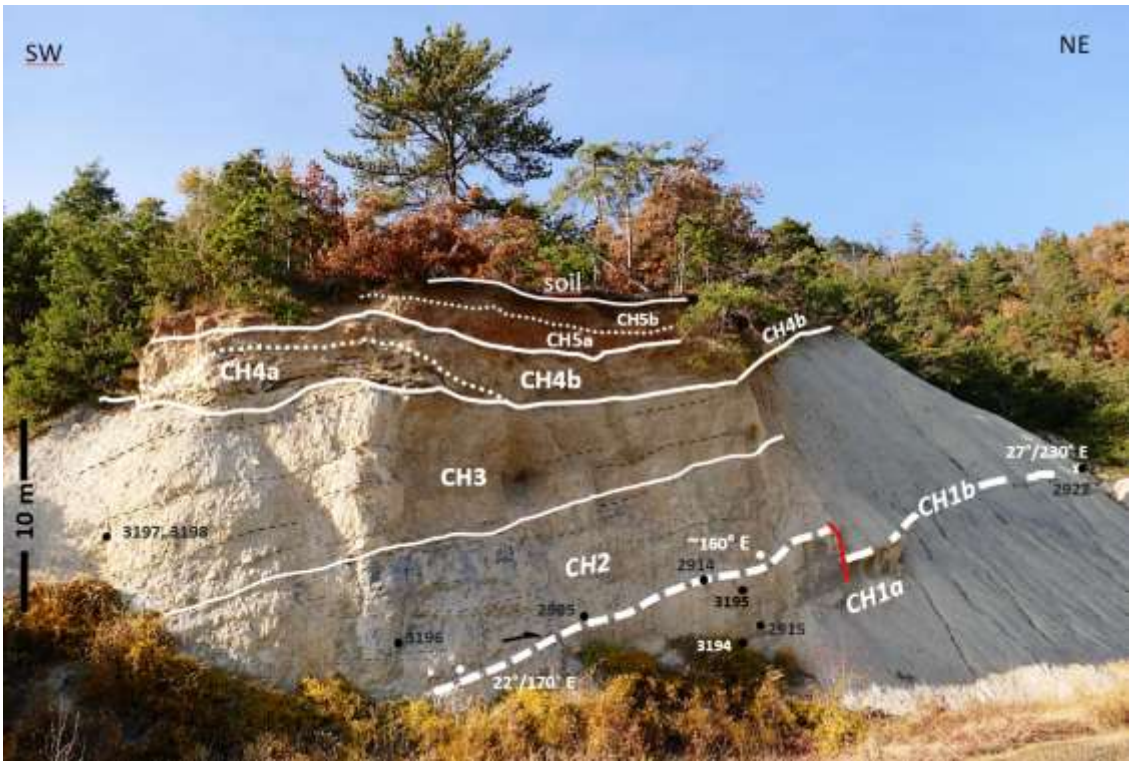

Fig. 4 Stratigraphy of the CH body (discussed in the text). The black arrow points to the "pseudo-onlap" of CH2 on CH1b. Numbers refer to analyzed samples. UTM coord. 2'600´730/1´124´430.

4.3.2 Sedimentology and petrography

The stratigraphy and the structure of the CH body of *SD* are shown on Fig. 4, whilst their sedimentological characteristics are detailed in Fig. 5.

The **CH1a** sub-unit is a stack of slightly indurated, grey-beige *DFD* composed of limestone and subordinate calcite and milky quartz pebbles embedded in a gravelly-sandy-clayey matrix (Figs 6b, 7 and 8). Apart from the dominant clay fraction, the latter includes authigenic calcite micro-crystals, minerals derived from RG moraines (clear quartz, rare fresh biotite, muscovite, tourmaline and zircon) and clasts of milky quartz, grey limestone, calcite, dark grey fine grained rounded limestones, calcschists, fine-grained quartz sandstones, gneiss and granodiorite. The limestone component originates from the Lower Jurassic of the Wildhorn Nappe, the sandstone from the Bajocian of the same nappe, the sandy limestone from the Penninic Couches de St Christophe (Badoux et al. lit. cit.). The undetermined clay-minerals could obviously not be related to a particular source and/or late transformations. Plant, gastropod and insect remains are present in small amounts (Fig. 18). At the top, decimeter-size flat components are lined up parallel to the stratification (Fig. 6a), a feature known in *DFD* (Corominas & al. 1996).

The compositionally similar, 5 to 10 cm thick **CH1b** conglomerate is poorly sorted and cemented by calcite. The early micritic and later sparry generations are indicative of atmospheric exposure (vadose environment, Scholle 1979) and carbonate-rich running waters, as does its upper smooth surface (Figs 6c and 6d).

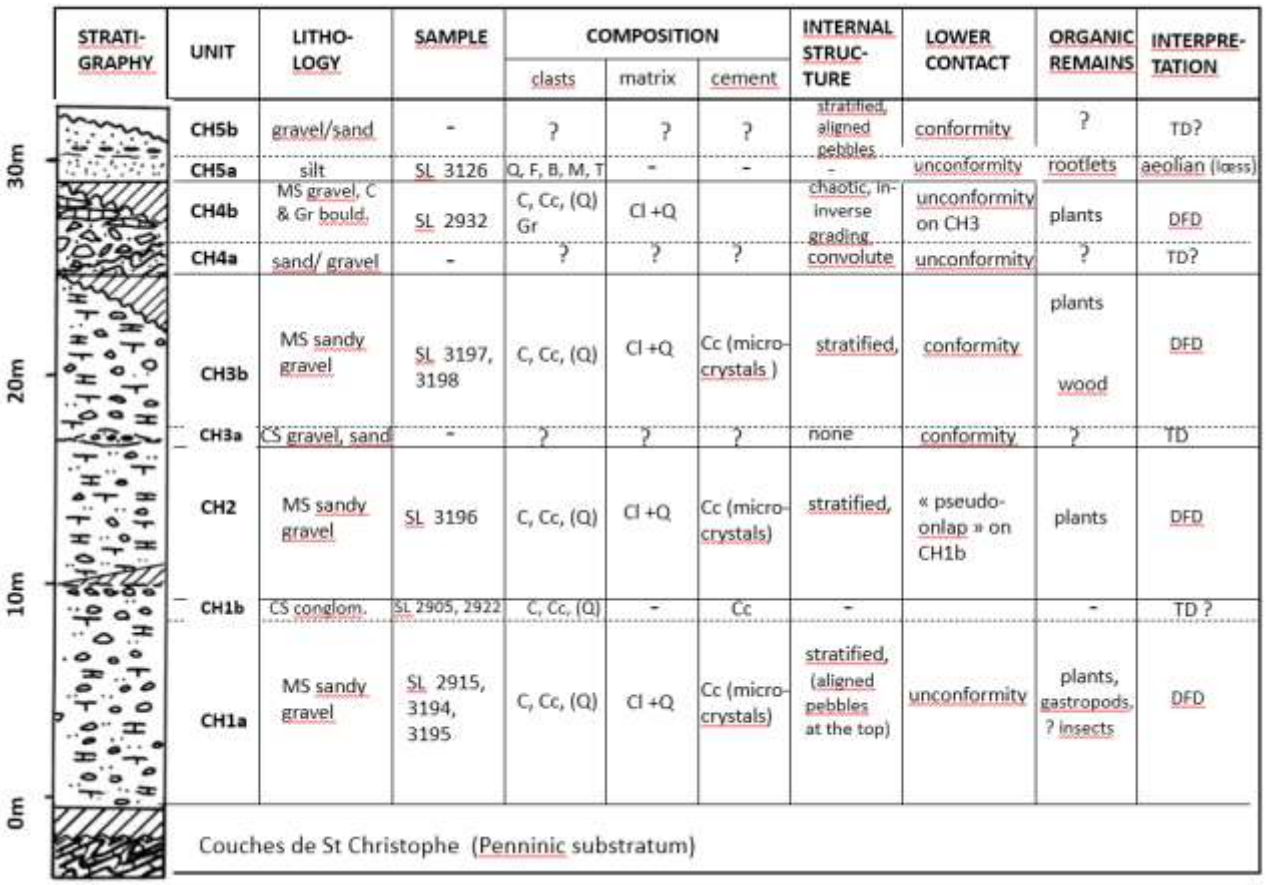

STRATI-GRAPHY	UNIT	LITHO-LOGY	SAMPLE	COMPOSITION			INTERNAL STRUC-TURE	LOWER CONTACT	ORGANIC REMAINS	INTERPRE-TATION
				clasts	matrix	cement				
	CH5b	gravel/sand	-	?	?	?	stratified, aligned pebbles	conformity	?	TD?
	CH5a	silt	SL 3126	Q, F, B, M, T	-	-	-	unconformity	rootlets	aeolian (loess)
	CH4b	MS gravel, C & Gr bould.	SL 2932	C, Cc, (Q) Gr	Cl +Q		chaotic, in-inverse grading	unconformity on CH3	plants	DFD
	CH4a	sand/ gravel	-	?	?	?	convolute	unconformity	?	TD?
	CH3b	MS sandy gravel	SL 3197, 3198	C, Cc, (Q)	Cl +Q	Cc (micro-crystals)	stratified,	conformity	plants wood	DFD
	CH3a	CS gravel, sand	-	?	?	?	none	conformity	?	TD
	CH2	MS sandy gravel	SL 3196	C, Cc, (Q)	Cl +Q	Cc (micro-crystals)	stratified,	« pseudo-onlap » on CH1b	plants	DFD
	CH1b	CS conglom.	SL 2905, 2922	C, Cc, (Q)	-	Cc	-		-	TD ?
	CH1a	MS sandy gravel	SL 2915, 3194, 3195	C, Cc, (Q)	Cl +Q	Cc (micro-crystals)	stratified, (aligned pebbles at the top)	unconformity	plants, gastropods, ? insects	DFD
		Couches de St Christophe (Penninic substratum)								

Fig. 5 Main properties of the CH units. C carbonate, Cc calcite, Q quartz, Gr granodioritic, Cl clay, CS clast-supported, MS mud-supported. The loess may overlie any of the older units. Vertical thicknesses.

The 7 m thick **CH2** unit (Figs 7, 9 and 10a) is a grey blue stack of decimeter thick, normally graded *DFD* including some thin clast-supported gravels interpreted as torrential deposits (*TD)* (Recking et al. 2013; Beauchamp 2020). Aalenian shales of the Wildhorn Nappe were most probably at the origin of the blue tint, which oxidation superficially turned to beige (Figs 4 and 10). Reddened sandstone clasts, and plant and insect debris are present in small amounts. The “pseudo-onlap” of CH2 on CH1b, suggests a lobate structure.

The beige, slightly indurated **CH3** unit consists of the thin **basal CH3a** *TD* (Fig. 10a) and of the overlying 4 to 12 m thick **CH3b** stack of *DFD* (Fig. 10) that is similar to CH2 in all its petrographic and sedimentological aspects (Fig. 7). The assumed pervasive oxidation has yet to be demonstrated. The matrix includes reddened clasts and rare plants remains of which a piece of wood (Fig. 18).

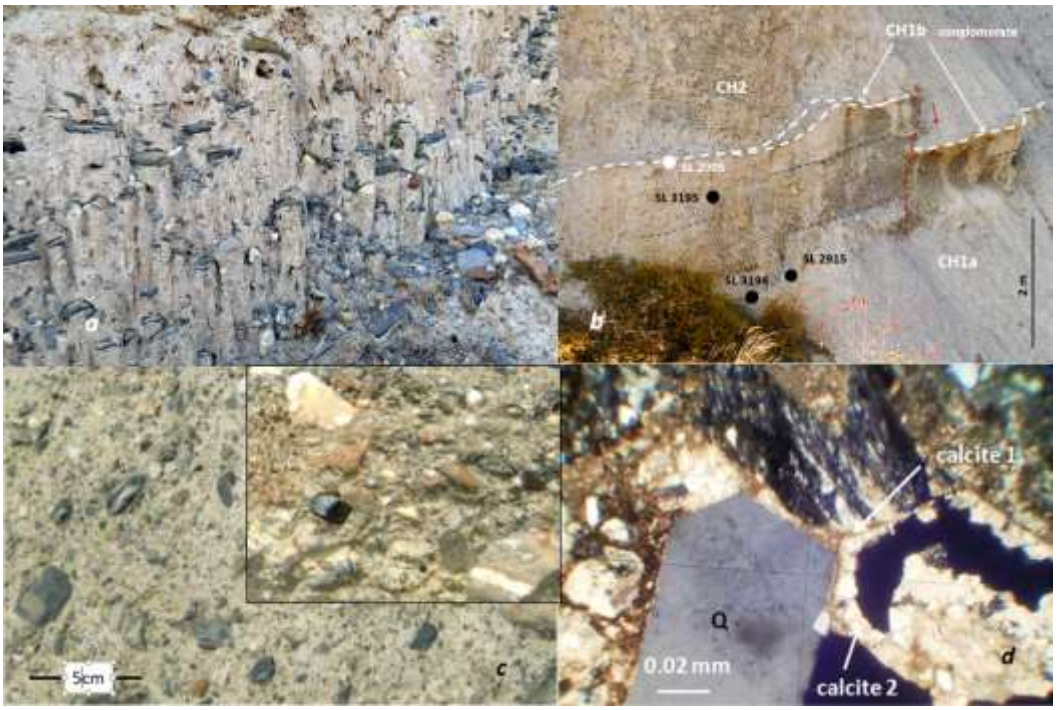

Fig. 6 *a* Alignment of pebbles at the top of CH1a; *b* Stratified top of CH1a. Folding and fracturing of the CH1b; *c* Smooth upper and lower rugged (framed) surface of CH1b ; *d* Micritic (calcite 1) and sparry (calcite2) cement of CH1b.

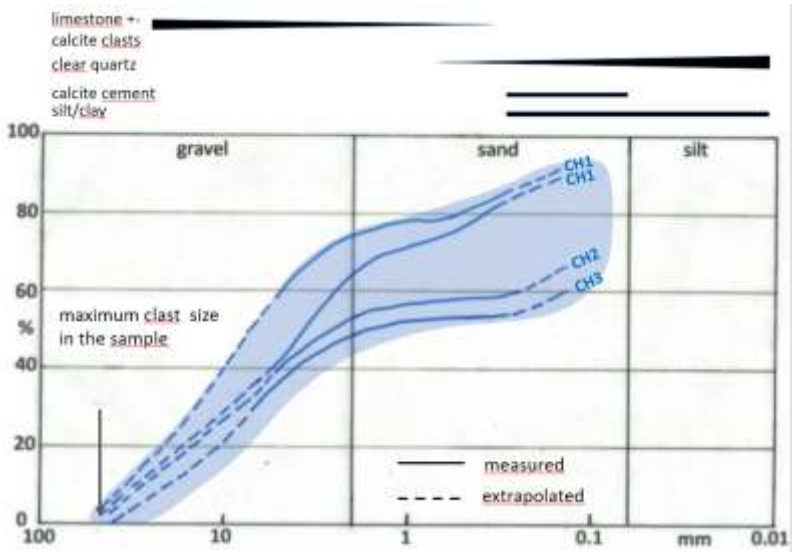

Fig. 7 The broadly logarithmic shape of the CH gravels grading curves suggests bulk transport of debris-flow type (Tricart 1965). The thickness of the black lines expresses the abundance of the component(s).

Fig. 8 CH1a. Rare limestone cobble embedded in a gravelly-sandy-clayey matrix.

Fig. 9 CH2. Superficial oxidation and desquamation.

The inaccessible, up to 2m thick grey beige **CH4a** lens of contorted sand/sandstone is interpreted as a partly cemented slice of kame terrace (Fig. 10b).

The overlying **CH4b** member is comprised of

- 1 to 4 m thick, grey beige, chaotic *DFD* of boulders and cobbles embedded in a matrix similar to that of the underlying *DFD*. The inverse grading observed at one point (Fig. 11) is a known feature of *DFD* (Nemec & Steel 1984; Costa 1984). Smoothed calcite encrusting of clasts points to reworking, possibly of cemented kame terrace clastics;

- an overlying imbrication of meter size sandy limestone slabs torn from the Couches de St Christophe and RG granodiorite and gneiss boulders/cobbles derived from RG moraine (Figs 10c and 12), whose structural arrangement clearly indicates the sense of emplacement.

The 4 m thick, brown **CH5** unit is comprised of a basal layer of brown **loess** silt (**CH5a**) overlain by an inaccessible gravelly sand (**CH5b**) with pebbles aligned parallel to the basal contact (Fig. 10d).

Fig. 10 *a* 20 cm thick CH3a *TD*; *b* Contorted CH4a lens; *c* Imbricated sandy limestone slabs and RG boulders at the top of CH4b; *d* CH5a loess and overlying and CH5b gravel.

Fig. 12 CH4b. Imbricated sandy limestone slab and granodiorite boulder.

Fig. 11 Inversely graded CH4b *DFD* underlying a slab of sandy limestone.

4.4 Valençon

4.4.1 General description and structure

At Valençon, Burri (1958) mentions « moraines non-stratifiées » about 30 m thick and probably deposited by local glaciers. Morphologically, the VAL body is an elongated bulge perhaps reaching the RV floor (Fig. 2). The constituting *DFD* and subordinate *TD*, which dip at about 25° towards SE, are exposed on a 220 m long, post-loess cliff (Fig. 13) and extend over 630 m from 700 to 630 m altitude (Figs 2, 13 and 14). The dips of the substratum layers exposed nearby vary from 40° to 50° and are directed towards SE, whilst their eroded surface dips at about 20° in the same direction.

Fig. 13 Down slope dipping VAL1 and VAL2 stacks of *DFD* and subordinate *TD,* unconformably overlain by VAL4. UTM coord. at the cliff center 2'602'270/1'124'590.

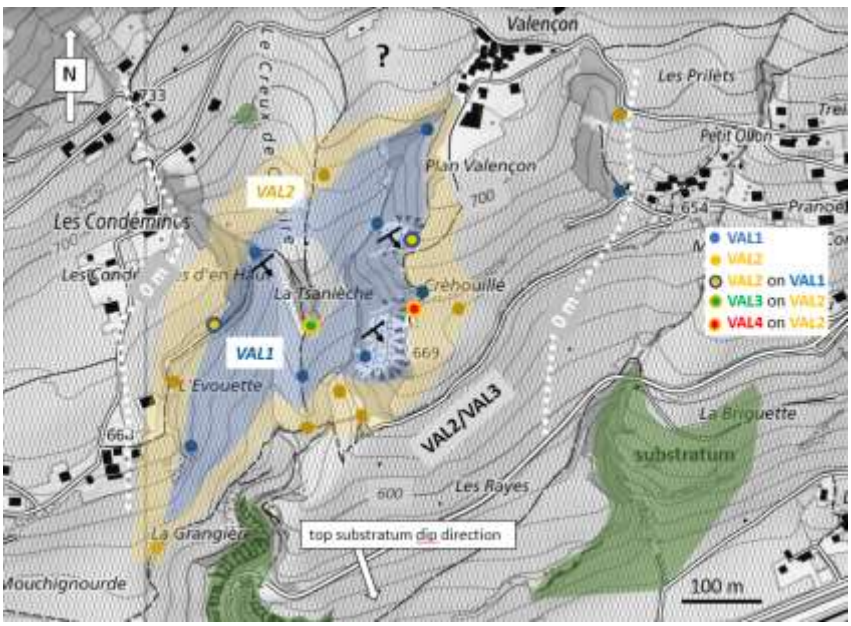

Fig. 14 VAL body geological map with selected stratigraphic control points (coloured dots) and 0 m isochores (white dotted 0 m lines, from the actual surface to the presumed, smoothed top substratum). The northern extension of the body is unknown, whilst the southern one probably reaches the RV floor. VAL3, identified on a spur separating two gullies, may be present on VAL2 on the western and eastern sides of the body below the vineyard soil.

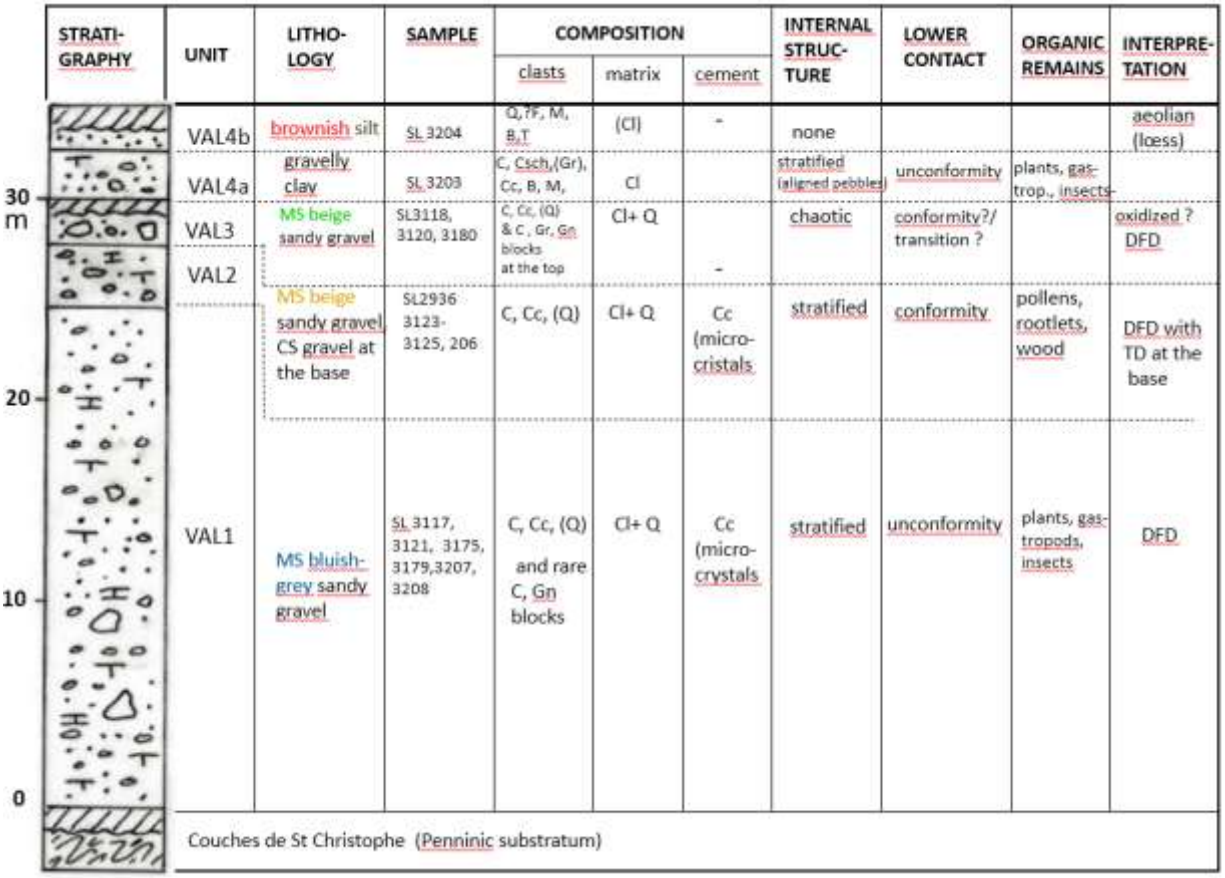

Fig. 15 Main properties of the of VAL units. C carbonate, Cc calcite, Q quartz, Gr granodioritic, Cl clay, CS clast-supported, MS mud-supported. Colours refer to control points on Fig. 14.

4.4.2 Sedimentology and petrography

The VAL body, which is comprised of the VAL1, VAL2 and VAL3 units/stacks of *DFD* and subordinate *TD*, rests on the Penninic substratum exposed nearby and is unconformably overlain by the VAL4 gravel and loess unit. The main sedimentological characteristics are presented in Fig. 15.

Congruently with the interpretation of the grading curves of selected samples (Fig. 17), the monotonous, grey blue **VAL1** unit is a stack of decimeter thick *DFD* (Figs 13 and 16). Its top is defined by the advent of the basal VAL2 coarse *TD*, which coincides with a colour change to beige. Some inverse grading is observed. The coarse components are mostly centimeter, rarely decimeter and exceptionally meter size (gneiss, limestone, weathered granodiorite) and predominantly comprised of greyish angular limestones with minor calcschists, vein calcite, gneiss, granodiorite and milky quartz (Fig. 17). The sandy-clayey matrix includes clear quartz, authigenic calcite microcrystals and some unaltered pyrite crystals. The latter were probably inherited from the Aalenian shale of the Wildhorn nappe (Massaad 1973) which also provided the grey blue clay. Scarce remains of plants, gastropods and insects are also present in the matrix (Fig. 18).

The beige, 0.5 to 3 m thick **VAL2** unit rests conformably on and is compositionally similar to VAL1 (Fig. 17), but includes beds of coarser components. The basal *TD* is mostly comprised of rounded, occasionally aligned, limestone pebbles and cobbles (Fig. 16b). The beige colour seems to be pervasive which would imply that oxidation took place before the mobilization of the debris. Locally, VAL2 erosional top has undergone a calciferous weathering not further investigated (Fig. 13). Organic remains include pollens, twigs and scarce carbonized wood. Frequently encrusted pebbles and grains indicate that older deposits were mobilized too.

The poorly exposed, a few meters thick, beige, chaotic **VAL3** unit is comprised of decimeter to meter size boulders of limestone, gneiss, fresh/weathered granodiorite and granite embedded in a gravelly-sandy-clayey matrix.

Fig. 16 *a* VAL1 *DFD* ; *b* VAL2 coarse basal *TD* and unconformable contact with VAL4.

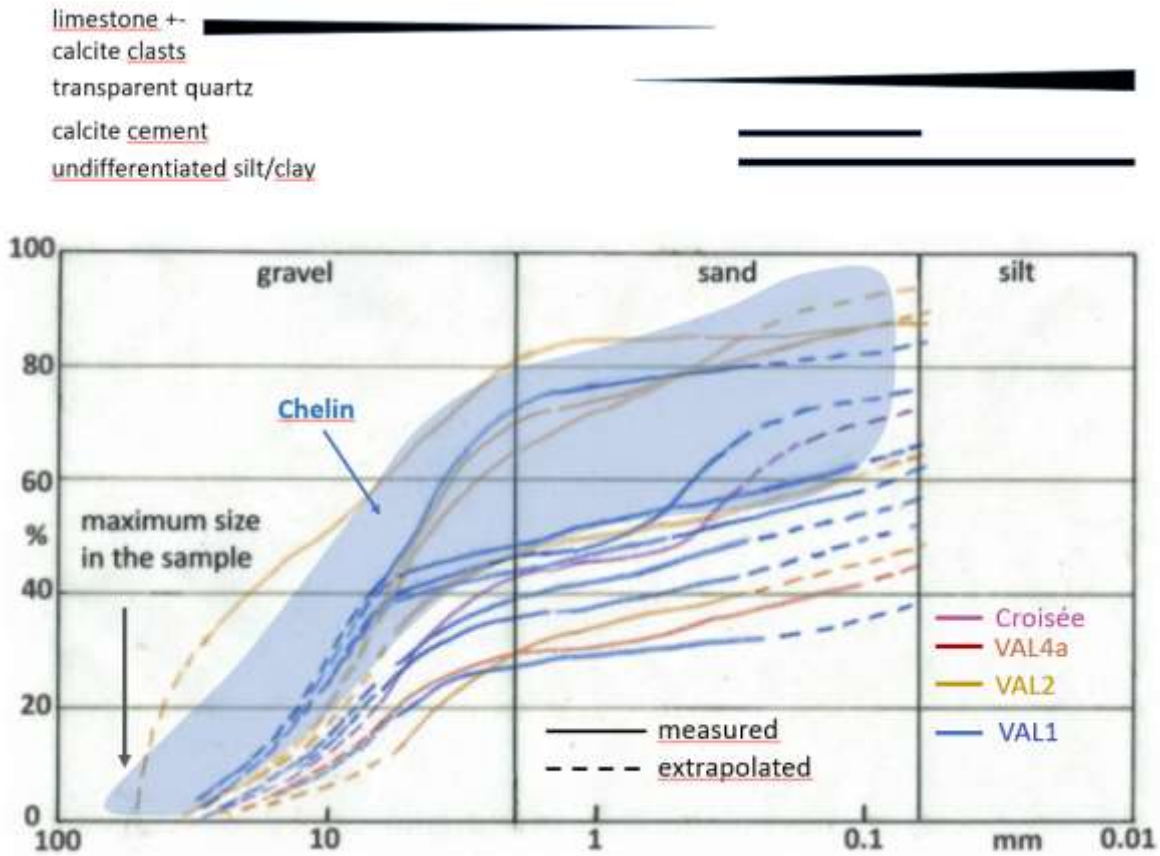

Fig. 17 Grading curves of the VAL and Croisée *DFD*. The thickness of the black lines expresses the abundance of the component(s).

Fig. 18 CH and VAL organic remains. *a* Twig; *b* Unspecified plant debris; c Gastropod, *d* Insect.

VAL4a is a brown, 0.8 m thick gravely gravelly clay with pebbles aligned parallel to the basal unconformity. The shape of its grading curve suggests that it is a *DFD* too (Fig. 17). The up to 10 cm large clasts include limestones, calcschists and rare milky quartz, as do those of the sandy fraction. Most pebbles and grains are encrusted by calcite. The abundant remains of gastropods and plants also include an insect chrysalis. Clear quartz, biotite, muscovite and tourmaline within the silty fraction may herald the deposition of the VAL4b loess.

The overlying thin (0.3 m) **VAL4b loess** silt rests conformably on VAL4a. Rare limestone and calcschist clasts and plant and mollusc remains, perhaps inherited from VAL4a, are associated with the typical loess minerals.

4.5 Croisée

The few meters high, Croisée exposure is comprised of grey blue, superficially grey beige, *DFD* of VAL1 type (Fig. 17), which include remains of plants and insects, as well as centimeter size gastropods. A VAL3 equivalent was probably also deposited, as suggested by the numerous granodiorite and gneiss blocks within the vineyard walls.

4.6 North flank: discussion and conclusions

The deposits

The CH and VAL bodies predominantly consist of monotonous stacks (CH1, 2, 3; VAL1, 2) of mud-supported gravel beds including subordinate clast-supported gravel streaks/beds interpreted as *TD*. Characterized by down-slope dip, normal and rare inverse bed grading, logarithmic grading curves and mainly local sourcing, the MSG are interpreted as *DFD* following Tricart lit. cit.; Costa 1984; Coussot et al. 1996; Corominas et al. 1996; Sohn et al. 1999; Leleu 2005; Cojan et al. 2006; Chambon et al. 2013; Bardou et al. 2013; Silhan et al. 2010; Novak et al. 2018.

The CH and VAL stacks of *DFD* are both overlain by a layer of chaotic mud-supported gravel (CH4b and VAL3) also interpreted as *DFD*. At CH, the latter overlies a contorted sand/sandstone interpreted as slice of kame terrace and is underlain by an imbrication of RG boulders and substratum slabs torn from the surface by catastrophic flush-flooding. The pervasively beige, oxidized *DFD,* are enriched in RG moraine components such as clear quartz grains, gneiss and fresh and weathered granodiorite boulders.

A broadly similar petrographic composition is shared by all the *DFD* and *TD*, with limestone components vastly predominating.

Environment and process of deposition

Although characteristic morphological features are not identified, the CH and VAL bodies are interpreted as remnants of individual alluvial fans, which would account for the local sourcing, the down-slope dips, the nature of the deposits (mainly *DFD* stacks), the lobate structure of CH, the similarities with confirmed fans on the opposite side of the RV and the presence of *SD* below the RV floor on nearby seismic data (Besson et. al. lit. cit.).

The emplacement of the VAL *DFD* was a rather continuous process, whilst that of the CH's was interrupted by iatus related to the cementation of the CH1b conglomerate, the CH2 pseudo onlap on CH1b and the probable colour change at the CH3-CH2 contact. In the absence of additional evidence, the origin of these different depositional stories remains speculative.

Extension of the fans

The original lateral extension of the fans is unknown but most probably exceeded the present one. The inter-fan areas, the soil composition of which reflects that of the fans (Canton du Valais 2007), were perhaps covered by unconfined *DFD* unless hypothetical fans were totally eroded. The CH and VAL fans very likely extended to below the RV floor as suggested by their significant thickness and by the vineyard soil composition adjacent to the RV floor.

Sedimentary sources and climate

The petrographic composition of all the *DFD* and *TD* indicates that formations of the Wildhorn nappe are the main primary source. The monotonous and thick *DFD* stacks must have required that large amounts of debris be funneled to the individual fans, a process that abundant precipitations and permafrost melting of rock glaciers would have allowed. The latters, which are known to have formed in the Alps between 13 and 8 ka BP (Scapozza 2012), are considered plausible secondary sources even though their location and the feeding channels are unknown. RG moraine and kame terrace scattered on the slopes and the substratum acted as limited sources which gained importance when the rock glacier source became exhausted.

The warm and humid climate is attested by the abundant water required for *DFD* generation, the pre-mobilization oxidation of the CH3?, CH4, VAL2 and VAL3 deposits and the presence of organic remains (insects, molluscs, plants), weathered granodiorite boulders and reddened clasts.

Fans' age

The timing of the fans' emplacement is poorly constrained between the disappearance of the RG and the deposition of the loess. The possibility to narrow this time span to the Late Glacial - Early Holocene transition is discussed in Chap. 5.5.

Sequence of events

The building of individual fans was followed by erosion, loess deposition and erosion.

5 The South flank

5.1 Geological framework

Regarding the Quaternary cover of that area, Burri (1997) states that "it is probable that the eroded masses above Les Fleurs 620-640 m) and perhaps the Ormeaux hill (715m) are lining successive edges of the RG" (author's translation). This interpretation of the Quaternary deposits which Gabus et al. (2008 a and b) took up in SGA sheet 111 (Fig. 24a) is considered erroneous.

The substratum consists of Carboniferous graphitic schists, meta-sandstones, meta-conglomerates and anthracite of the Zone Houillère (ZH), (Fig. 19a) (Christ 1925; Steck et al. 1999; Gabus et al. lit. cit.).

The Val de Réchy (VR) - Le Tsan (TSN) glacial cirque and the voluminous *SD* accumulated below 900 m are obviously connected (Fig. 19b). Within and along the VR and TSN crop out marmorized limestones and marbles of the ZH, gneiss, quartzite, chlorite-schists, meta-conglomerates, quartzitic schists, cellular dolomite, prasinites, ovardites of the Siviez-Mischabel (SM) nappe, which provided the bulk of the *SD* material, and schists, calcschists and marbles of the Tsaté (TS) nappe formations (Fig.19a) (Steck et al. lit. cit.; Marthaler et al. 2008). The flat/counter-slope dips of the layers combined with a large catchment area, a strong alpine fracturing and frost-defrost certainly favoured the massive production of clastic material which later constituted the fans Chap. 5.2).

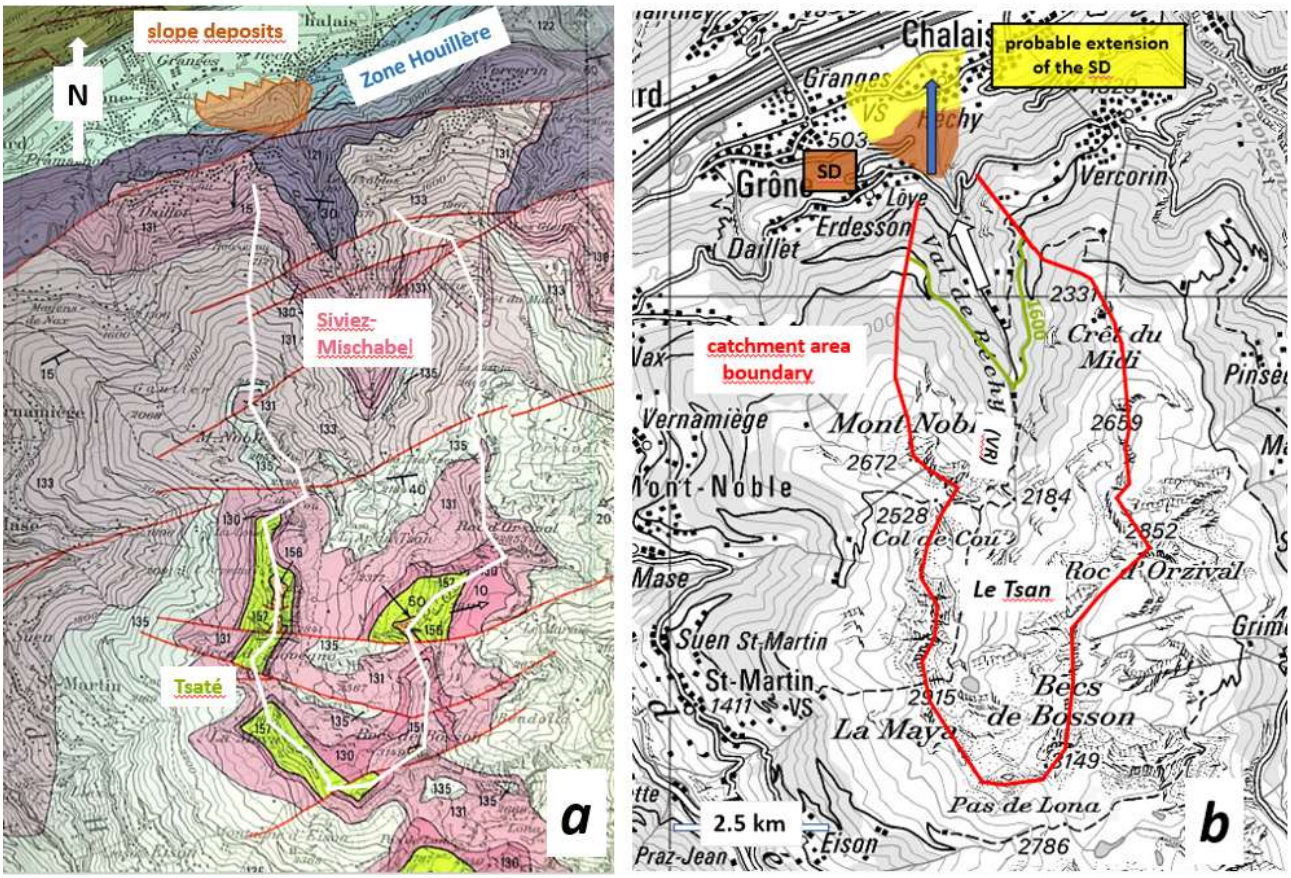

Fig. 19 *a* Tectonic framework of the area (excerpt of Steck et al. lit. cit.) in relation to the investigated *SD*. The Zone Houillère (Carboniferous and Triassic) is overlain by the SM nappe, itself overlain by the TS nappe.
b Topographical map of the same area. The Réchy gorge (blue arrow) incises the *SD* in a S-N direction which deviates from the VR trend below 1600 m (white arrow) (discussion in Chap. 5.2).

5.2 Morphology

The morphology of the investigated area essentially consists of the Creta Limbo (CL), Les Clous (CS), Les Fleurs + Les Ormeaux (FL+OR) units of Quaternary *SD* that are separated from each other by pre-loess ravines R1 to R10 (Fig. 20).

FL, the largest of the three units*,* currently covers an area of about 0.6 km^2 (vertical projection) from 500 to 900 m and displays the conical shape and a hemi-circular intersection with RV floor characteristic of an alluvial fan. Its eastern flank is deeply incised by the Rèche river (RR) gorge or R4 ravine. The latter's S-N trend, for unknown reasons, deviates from the NW direction of the Val de Réchy (VR, Fig. 19b), of the R1, 2, 5, 6, 7, 10 ravines (Fig. 20a) and of the OR landslide track (Chap. 5.4. On the western side, FL's surface S9 is truncated by the S1 planar surface (associated to R1) which up-slope projections are truncated by S4. FL is partly overlain by the Réchy alluvial fan built during the carving of the RR. The large blocks (up to tens of cubic meters) scattered on S4 and within the RR gorge were presumably deposited on FL's original surface and later redeposited.

Resting on FL and characterized by counter-slope dipping layers, the slab-shaped **OR** unit is the remnant of a large landslide (Chap. 5.4 and Fig. 47). It is truncated by the S2 and S3 planar surfaces still preserved on top of the Ormeaux cone (Fig. 51) and by cliffs later carved in those.

The contiguous **CL** (now erased) and **CS** units, interpreted as remnants of alluvial fans, are limited by ravines R5 to R8. The saddles at the southern extremities of late CL and current CS, which are situated at different altitudes, could represent the original apexes of separate fans coalescing down-slope and siding with FL. Before its exploitation, **CL** was an imposing tongue dominating the RV floor by some 70 m (Fig. 19*b*), limited by R6 and R7 whose associated smooth S7 surface was still visible in the early 90ies (Fig. 21). **CS** is a narrow tongue with rather steep slim flanks, whose short longitudinal extension probably results from the merging of the R1 and R8 ravines.

In short, below about 1000 m the landscape was successively shaped by the carving of the RV flanks, the emplacement of the FL, CS and CL fans, their partial erosion, the building of the Réchy fan and the post-loess consolidation.

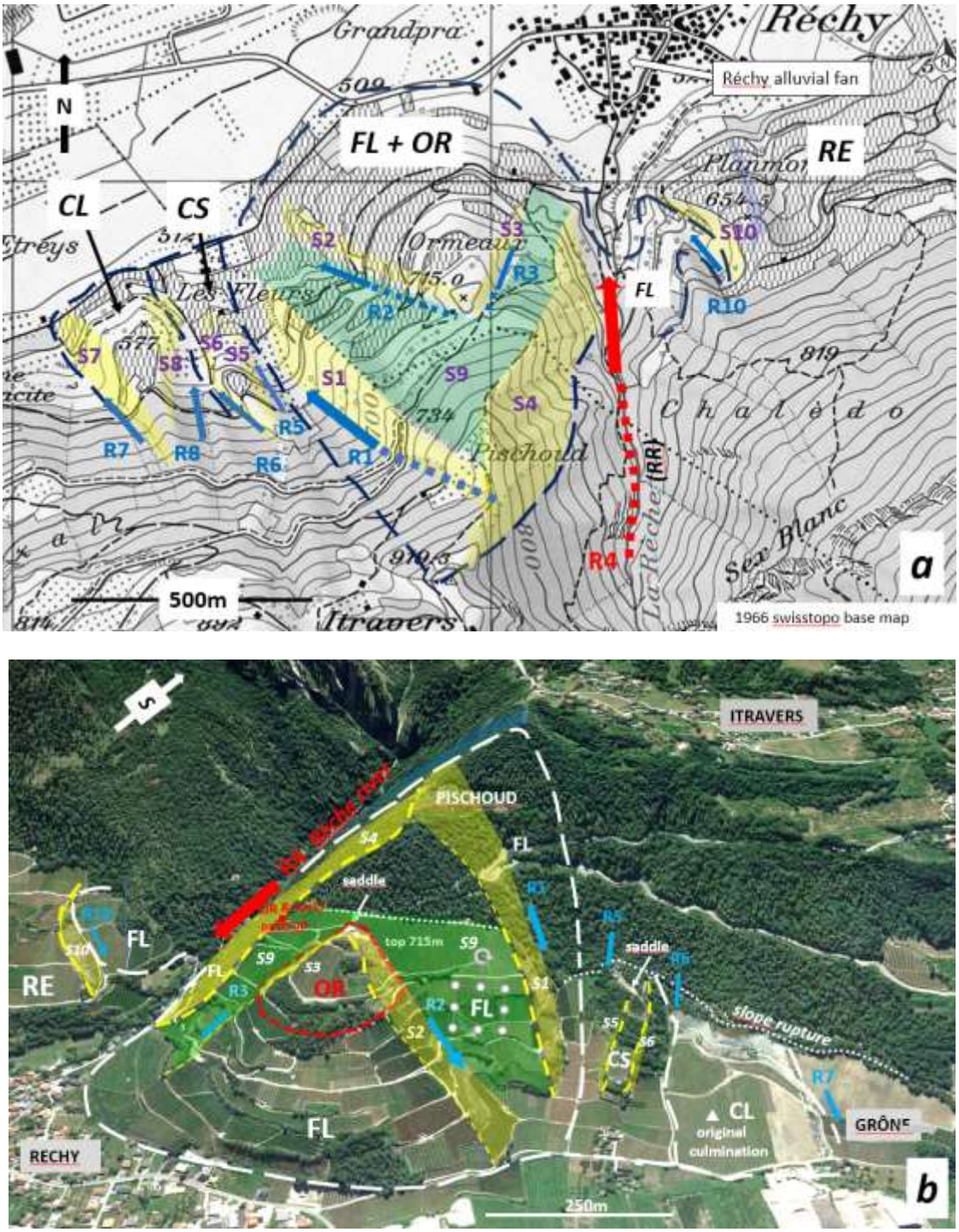

FIG. 20 *a* Boundaries of the CL, CS and FL+OR morpho-geological units (dashed dark blue lines). R1/S1 … refer to ravines and associated actual or residual planar surfaces (yellow shaded) as in Fig. 20b. RE stands for Réchy and covers the area situated between FL's eastern edge and the Tsararogne quarry (Fig. 1). Google Earth side view.
b Google Earth side view of the investigated S flank. Same elements as above with cuestas added (dashed yellow lines, thick if sharp).

Below 700 m, from FL's eastern edge to the Chalais and Tsararogne quarries, the flank is less rugged due to the general thinness of the Quaternary cover which Gabus et al. (lit. cit.) labelled "Moraine de la dernière glaciation" on SGA sheet 111 (Figs 1 and 23). According to the present author's unpublished observations, this cover is comprised of *SD* and not moraine, which agrees with the down-slope dipping gravels and sands reported by Burri (1997) in those quarries, but associated by him to the RG.

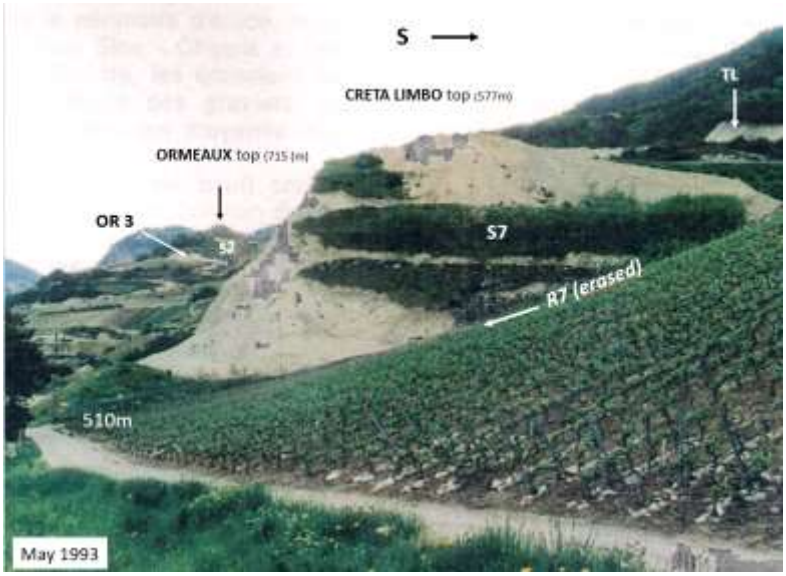

Fig. 21 CL's western, sliced planar flank S7, the pre-loess age of which is attested by the presence of loess at higher altitude.

5.3 Geology of the Creta Limbo, Les Clous and Les Fleurs units

Whilst the superficial geological control is fair, the deeper structure and sedimentology are unevenly if not poorly controlled (Fig. 22).

5.3.1 General description and structure

With their constitutive *SD* dipping towards the N-NW, the **FL** fan and the **CL** and **CS** fan remnants thicken and widen down-slope and certainly contribute to the filling of the RV (Figs 23 to 28). In the case of the CL fan, departures from these directions suggest a lobate structure (Figs 29 and 30). Outside of the OR landslide the fans' surfaces, are smooth and disturbed by few superficial faults only (Figs. 31 and 32).

As suggested by the horizontal projections of its emerging hills against the slope, the Sierre landslide (SL) most probably overlies the fans (Fig. 26). Were this not the case, the paleo-Rhône could not have deposited alluvions on the landslide surface (Burri 1997) since it would have flowed in the depression running between the landslide and the slope (and in other depressions). Whether SL lies below or above the Réchy fan is not known.

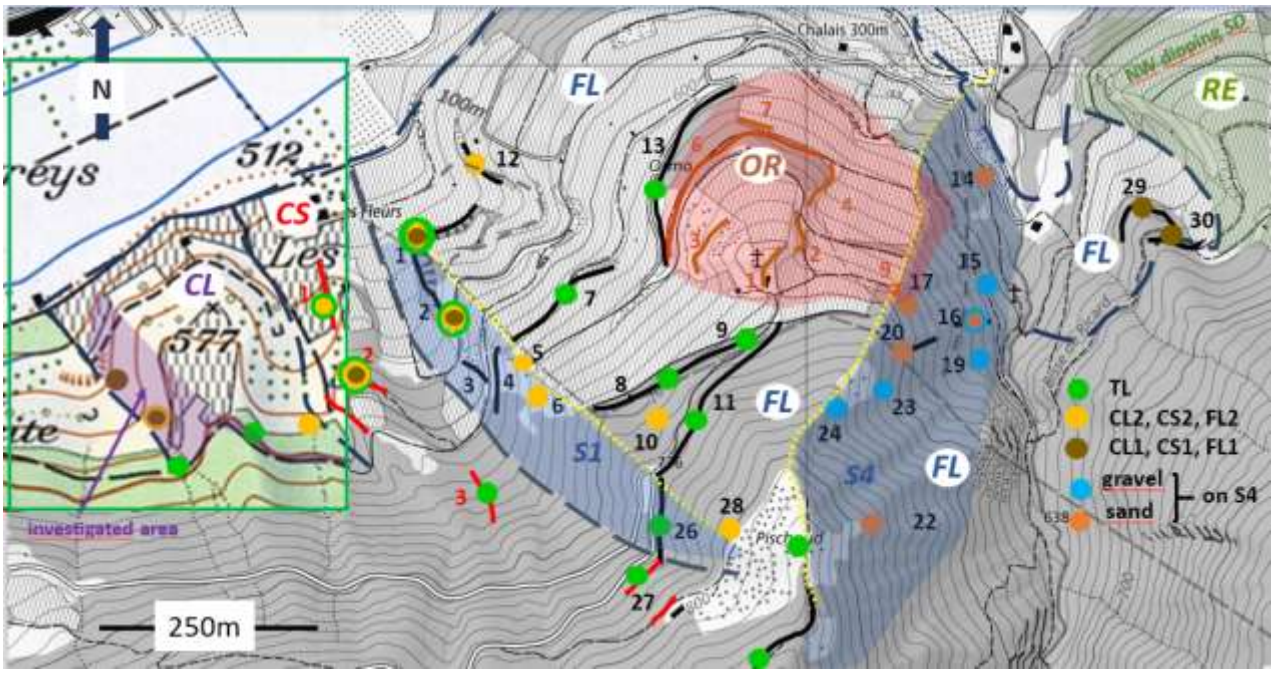

FIG. 22 Distribution and numbering of the CL, CS, FL and OR exposures. These are shown as thick lines if large and dots if small. The exposed units/lithology are identified by the dots colour. 2017 swisstopo base, 1966 within the green frame.

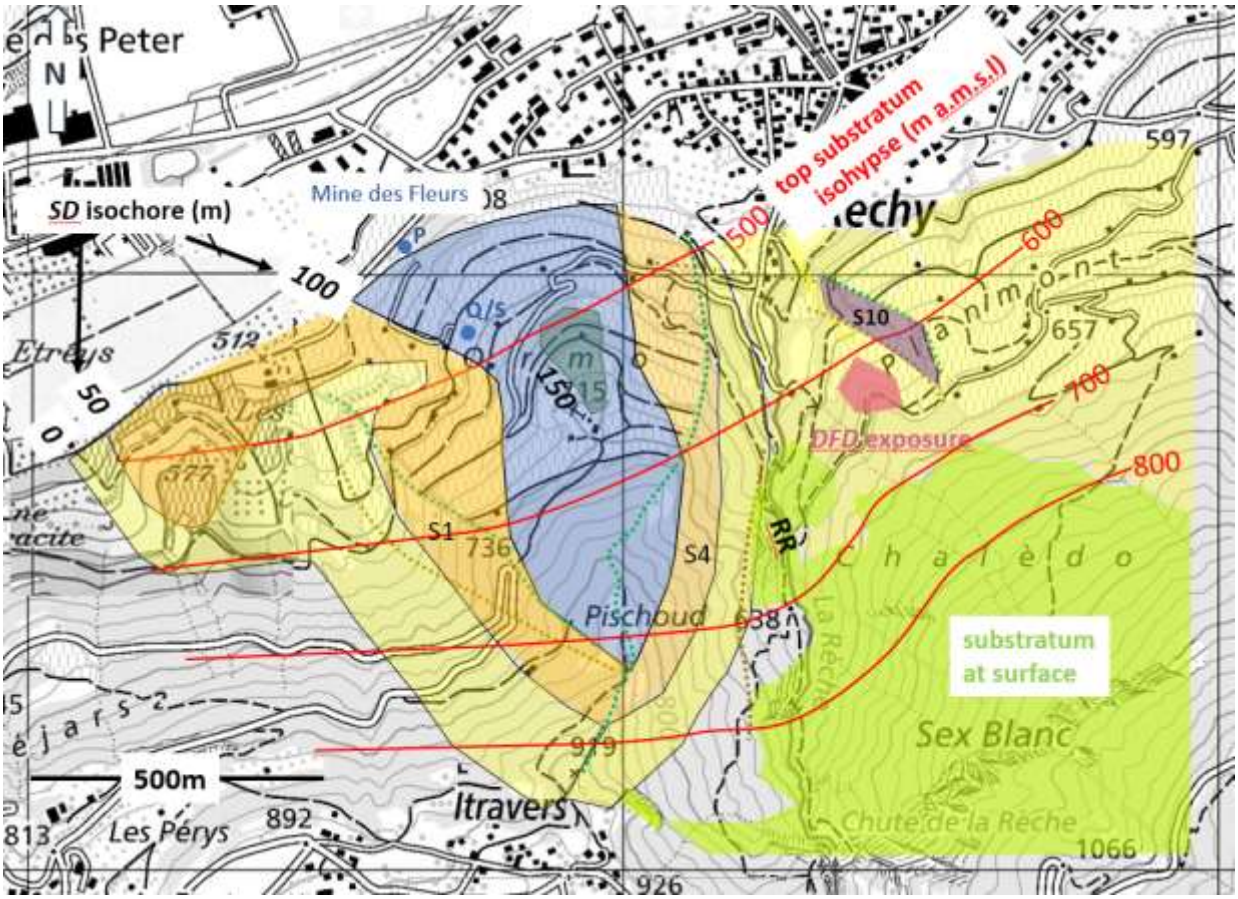

Fig. 23 Approximate isochores of the Quaternary cover. The S1 and S4 planar erosional surfaces are bound by cuestas (green dots) and bottom (brown dots). East of the RR, the cover thickness is well under 50 m, the *DFD* exposure marks the eastern limit of the FL fan and the S10 surface consists of slope parallel coarse gravel layers outside FL. The P to Q/S dotted blue line is the approximate trace of the Les Fleurs coal mine gallery where, according to Gabus et al. (lit. cit.) some 75 m of Quaternary overlie the substratum. This probably inaccurate figure has not been taken account in view of the "heavy" smoothing of the isochores and of the top substratum isohypses (Fig. 24). 2017 swisstopo base, 1966 over the CL fan (as in Fig. 22).

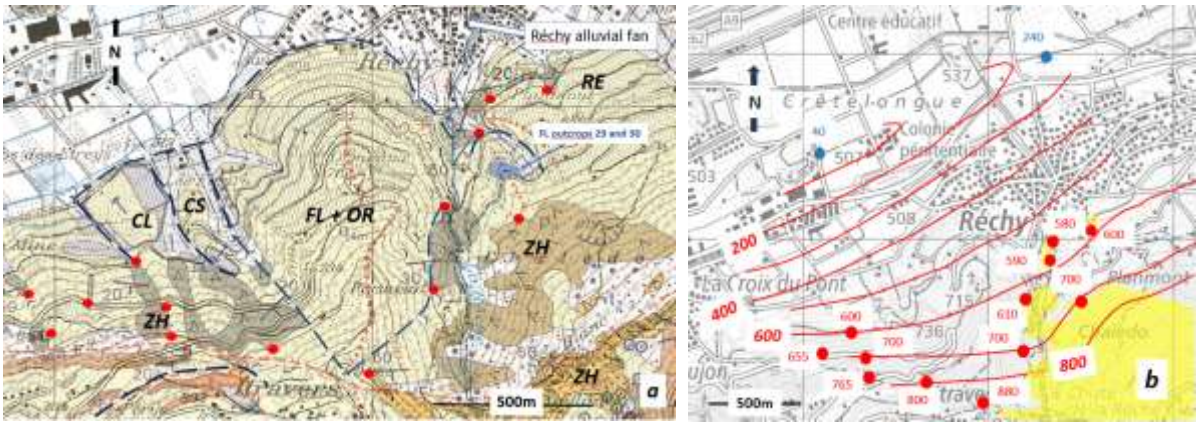

Fig. 24*a* Excerpt of SGA sheet 111 with the boundaries of the *SD* units (dashed blue lines) and the location (large red dots) of the Quaternary-substratum contacts used to construct the top substratum isohypses of Fig. 24b. Pale green area: moraine of the last glaciation with vallums (aligned small red dots) which are actually cuestas.
b Smoothed isohypses (m) of top substratum obtained by contouring a loose grid of gravimetrically derived altitudes of the RV axis (blue dots, Rosselli and Olivier lit. cit.) and altitudes of the Quaternary-substratum contacts (red dots). The yellow cloud shows substratum at surface along and E of the RR.

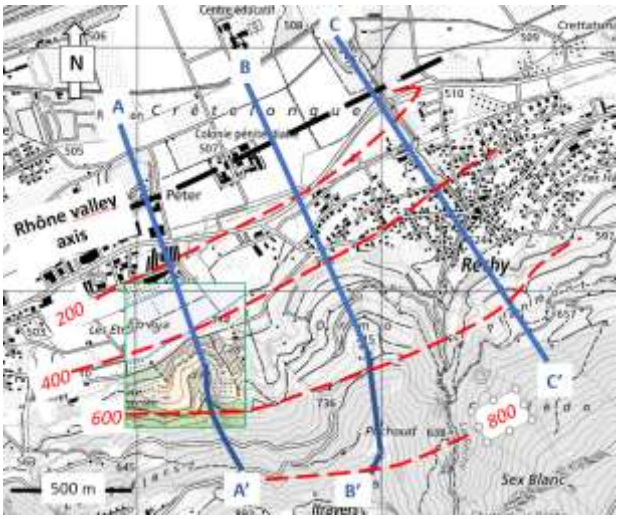

Fig. 25 Traces (blue lines) of the geological cross-sections of Fig. 26. Dashed red lines are top substratum isohypses. 2017 swisstopo base, 1966 over the CL fan.

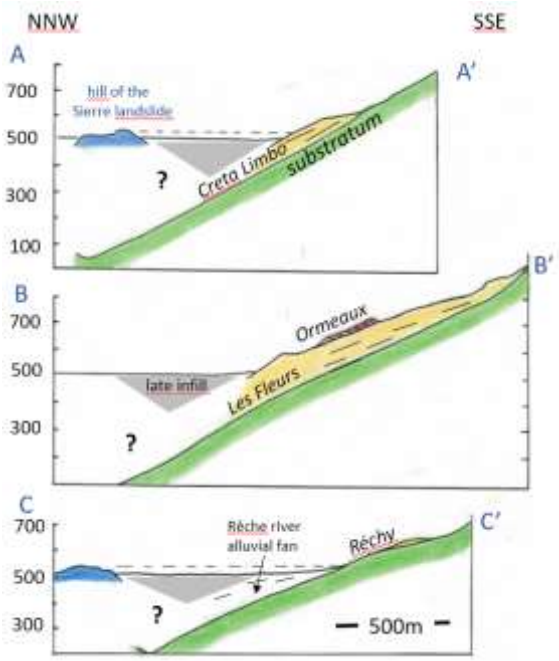

Fig. 26 Geological cross-sections along the traces of Fig. 25. The *SD* cover is yellow coloured, the Ormeaux slab brown. The horizontal projections (dashed black lines) of the SL hills come in contact with the Creta Limbo fan and the thin Réchy *SD.*

Fig. 27 Northerly dip of the CL1 *DFD* within the CL trench. Gneiss boulder ~3 m wide.

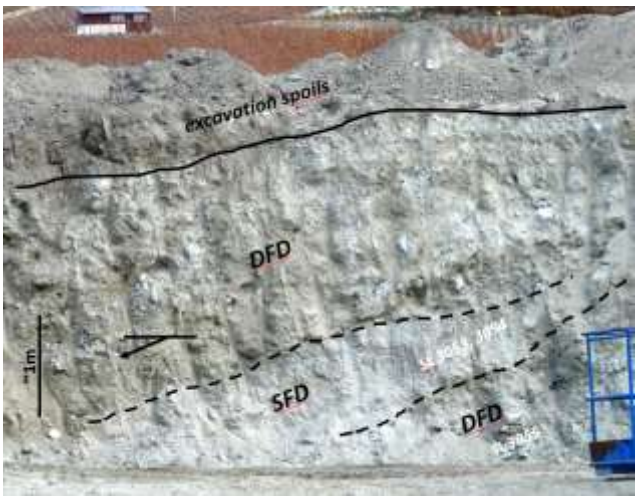

Fig. 28 Northerly dip of the CL1 *DFD* and intervening *SFD.* Northern extremity of the CL trench.

Fig. 29 Diverging dip directions of the CL1 *DFD*.

Fig. 30 Variable *DFD* dip directions (blue arrows) on CL's exploitation front.

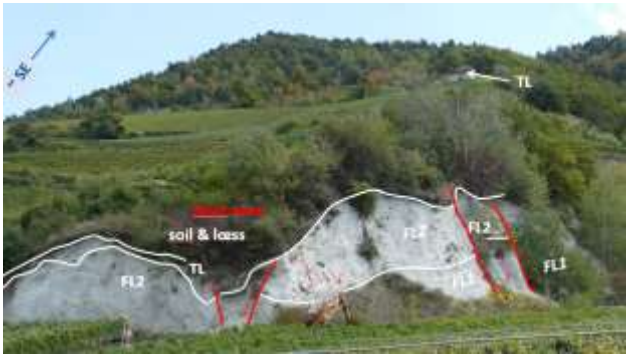

Fig. 31 FL's three member superficial sequence and late post-loess faulting. FL exposure 1, Fig. 22.

Fig. 32 Superficial fault. CS exposure 2, Fig. 22.

5.3.2 Stratigraphy, sedimentology and petrography

The exposed stratigraphic sequence - thick for CL, thin for CS and FL - is bottom-up comprised of:
- a stack of *DFD* (CL1, CS1 and FL1) with subordinate sand-flow deposits (*SFD)* and *TD,* conformably overlain by
- a layer of *SFD* (CL2, CS2, FL2) conformably/disconformably overlain by
- a Top Layer (TL) composed of chaotic, unstratified/coarsely stratified layers (TLa) conformably overlain on FL by stratified/unstratified gravels (TLb).

These members share both lithology and grading curves whereby the logarithmic shape of the gravels is characteristic of *DFD* and the sigmoid one of the sands indicates free accumulation (Tricart lit. cit.) (Fig. 33). Sources and processes are thus shared by all deposits.

The unexposed part of the fans, including that below the RV floor, presumably consists of deposits akin to those encountered within the CL trench and exposed on its exploitation front (Figs 22, 27 and 30). The isolated exposures on the S1, S2 and S4 surfaces, which span large parts of FL's inner section, neither infirm nor confirm this hypothesis (Fig. 22).

The *DFD*

The **CL1** member reached a 70 m thickness on the quarry front (Fig. 30) and 20 m in a side-trench (base not exposed in both cases). It was in the latter a stack of decimeter thick *DFD* including layers of *SFD* layers/beds (Figs 28 and 34), a single 1 m thick *TD* conglomerate (Fig. 35) and a decimeter thick sandy clay close to the base. Volumetrically insignificant, the latter two lithologies merely illustrate the variety and complexity of the processes involved in the fans' construction.

The thinner, less than 10 m thick **CS1** and **FL1** have no intervening *SFD* but are respectively capped by a layer of *TD* (Fig. 36) and 3 m thick alternation of gravel and sand.

The *DFD*'s centimeter to decimeter, rarely meter size components (up to tens of tons in CL1, Fig. 27) include angular chlorite-schists, gneiss, prasinites, massive and schistose quartzites (some with pink quartz), sub-angular gneiss and mica-schists, rounded limestones (recrystallized/marmorized), rare serpentinite, meta-conglomerate and Carboniferous carbonaceous limestones scraped from the substratum.

The argillaceous-sandy-gravelly matrix is comprised of the disintegration products of the coarse components and clay minerals. The amount of quartz, chlorite, muscovite, magnetite and rutile increases with decreasing grain size (Fig. 33). In line with the low induration, the calcite is detrital.

E of the RR gorge, at outcrops 29 and 30 (Fig. 22), a 6 m thick, coarsely stratified *DFD* stack (Figs 34d and 37) is overlain by 0.5 m of grey, clayey silt and 0.6 m of chaotic TL gravel, itself disconformably overlain by pebbly loess (Fig. 38).
The *DFD* pebbles and cobbles include quartzites, various gneiss, chlorite- and mica-schists and are frequently calcite encrusted. Its matrix is comprised similar lithologies, with white clay (kaolinite?), translucent/clear quartz and minor amounts of magnetite, rutile, chlorite and calcite concentrated in the less than 0.1 mm. fraction. Plant and insect remains are common.
The silt's coarse fraction is comprised of fine-grained limestone, quartzite, gneiss and chlorite-schist, whilst minute grains of quartz, calcite, muscovite, magnetite, rutile, chlorite, quartzite, chlorite-schist and gneiss constitute the matrix. Of interest for age dating, a basal veneer of white clay (kaolinite?) includes squeezed plants not connected to the soil (Figs 38 and 39).
The close resemblance of these *DFD* to FL1's, the thinness of the overlying silt, the proximity of FL across the RR gorge and the reduced thickness of the *SD* (Fig. 23) together strongly suggest that FL extends E of RR (Figs 19, 20, 22 and 23), however not much further E than outcrops 29 and 30.

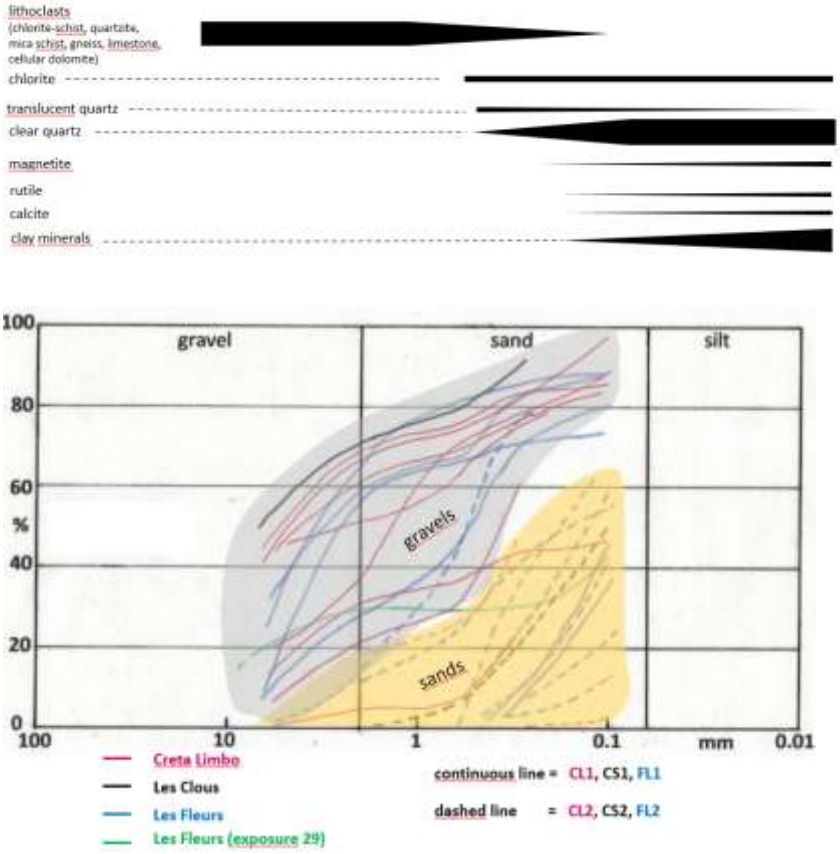

Fig. 33 Composition and grading curves of the CL, CS and FL gravels and sands. The latter form two families with few transitional terms (discussion in the text).

Fig. 34 Examples of *DFD*. *a* Within the CL trench, including a bed of *SFD*; *b* Coarsely stratified CS1 at CS exposure 1 (Fig. 22); *c* At FL exposure 1 (Fig. 22); *d* At FL exposure 29 (Figs 22 and 38).

Fig. 35 Conglomerate within CL1. Clasts are grey limestone (1), white quartzite (2), fresh (3) and altered (4) chlorite-schist. Translucent calcite provides the cement. The residual pores are lined with a rim of calcite micro-crystals indicating vadose cementation (Scholle lit. cit.). The latter did require an extended atmospheric exposure and running surface waters.

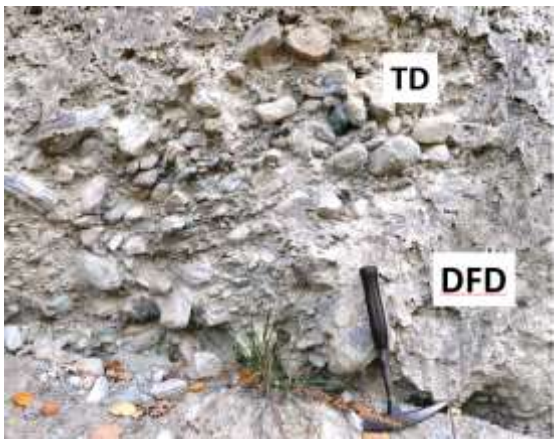

Fig. 36 *TD* on top of the CS1 *DFD.* CS exposure 2 (Fig. 22).

Fig. 37 Coarsely stratified *DFD.* FL exposure 30 (Fig. 22).

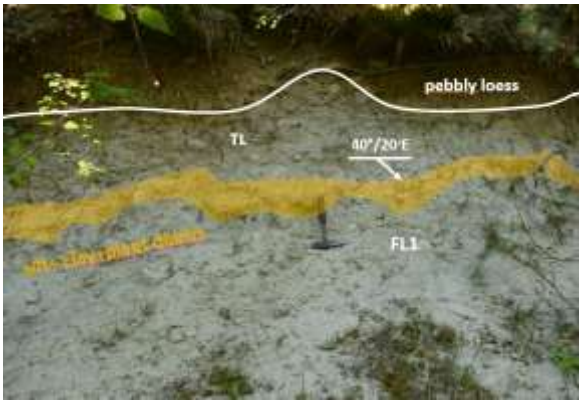

Fig. 38. FL stratigraphy. FL exposure 29 (Fig. 22).

Fig. 39 Squeezed plants. FL exposure 29 (Fig. 22).

The *SFD*

The **CL2, CS2** and **FL2** members are stacks of grey beige, millimeter thick laminae of very well sorted, very fine, slightly indurated sand (Fig. 40), whose total thickness reaches 8 m at FL exposure 1 (Figs 22 and 31) but is thinner elsewhere. The sand layers, laminae and intervening gravelly streaks always dip down-slope. It is assumed these laminae were emplaced as thin slurries and represent sand-flow deposits (*SFD*) similar to those described by Sohn et al. (1999).

Fig. 40 Examples of laminated CL2, CS2 and FL2 sand (*a, c* and *d)*, with parallel gravel streak in (*d)* and in clear contact with CS1 in (*b)*.

The TL

At FL exposures 8 and 9 (Fig. 22), **TL** comprises bottom-up

- the ubiquitous, chaotic/coarsely stratified **TLa** sub-member characterized by the abundance of decimeter to meter size gneiss and chlorite-schist boulders/blocks frequently encrusted by calcite, as are the coarser matrix components (Figs 41 and 42). The cobbles and pebbles include chlorite- and mica-schist, various gneiss, quartzite, meta-conglomerate, striated serpentinite, recrystallized/marmorized limestone, dolomite and cellular dolomite. The same lithologies and their disintegration products compose the gravelly-sandy part of the matrix, and
- a conformably overlying **TLb** sub-member, absent elsewhere, and consisting of a 1 to 5 m thick stack of fine to coarse stratified *TD* and *DFD* with intervening sand beds (Figs 43 and 44). Its petrographic spectrum is shared with TLa. Calcite encrusting, polished or not, and organic remains (e. g. insect paws) are frequent. The *DFD* include chunks of fine sand presumably scraped from FL surface and gravel blobs with limonitized matrix (Fig. 45).

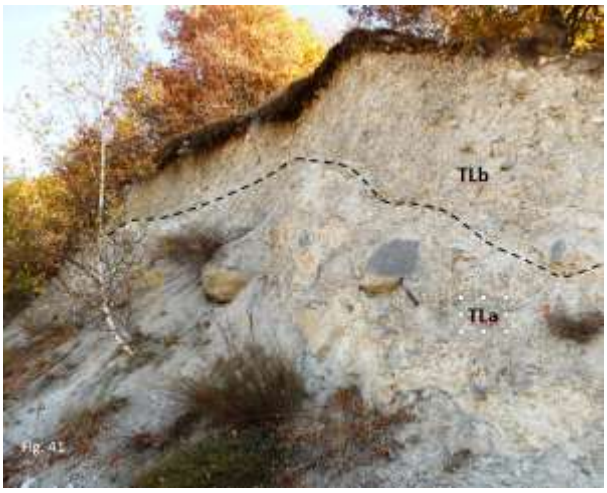

Fig. 41 TLa-TLb contact. FL exposure 8 (Fig 22).

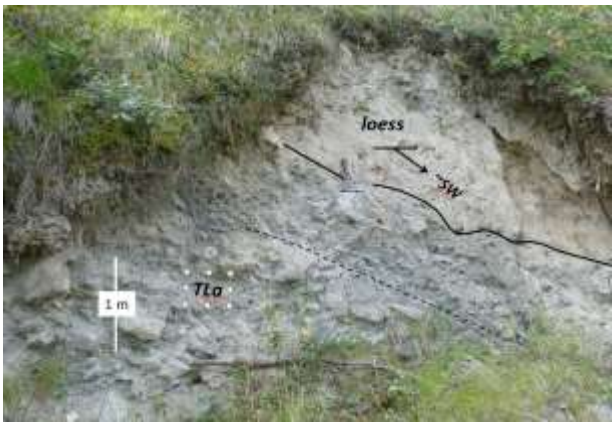

Fig. 42 Chaotic/coarsely stratified TLa underlain by loess. Road above CL (Fig. 22).

Fig. 43 TLb stack of decimeter thick clast- and mud-supported gravel beds. FL exposure 9 (Fig. 22).

Fig. 44 Fine-grained clast-supported gravel laminae within TLb. FL exposure 9 (Fig. 22).

The FL section on the S4 surface and opposite side of the RR

An over 100 m thick FL fan section occupies the mostly overgrown, very steep S4 surface (Figs 22 and 23). Loess deposited on this surface sets a maximum age for the carving of the RR gorge and the building of the RR fan (Fig. 46). The small size of the scattered gravel and sand outcrops (Figs 22 and 46) and the lack of reliable structural information preclude any litho-stratigraphic reconstruction and correlation with the sequence on the SW side of the FL fan. Long linear cracks and associated sliding could be at the origin of the variable dips and dip directions of the loess and underlying beds. According to the proposed OR emplacement model (Chap. 5.4.3), OR alternations could be present on top of S4.

On the opposite side of the RR, the FL fan thins to a few tens of meters or less below 700 m, whilst it has been totally eroded above.

Fig. 45 Chunk of sand within TLb and weathered *DFD* gravel blob. FL exposure 9 (Fig. 22).

Fig. 46 Isolated sand and gravel at FL outcrops 14, 15 and 24 on the S4 surface (Fig. 22) and TLa along the Itravers-Pischoud track (Fig. 20a).

5.4 Geology of Les Ormeaux unit

5.4.1 General description and structure

The ~ 230 m long and wide OR slab (Figs 20, 22 and 47) is laterally limited by the 10 to 20 m high S2 and S3 cliffs of demonstrably pre- and post-loess age (Chapter 5.2.). The isolated OR9 exposure suggests that OR extended to the SE over a domain later eroded by R4 (Figs 48 and 49). The southern current limit coincides with an erosional saddle. The north-northwestern one may be situated at or close to the actual slope rupture or to FL's exposure 13 where down-slope dipping gravels and sands could be attributed to either TL or to FL (Figs 22 and 48). The SW original extension is unknown but was certainly situated W of OR3. Assuming a smooth surface of FL, the exposed slab thickness reaches 30 m in the central part (Fig. 48). However, as discussed in Chap. 5.4.3, its total thickness (down to the unobservable base) most probably exceeds this figure.

OR consists of counter-slope dipping dissimilar gravel-sand alternations unconformably overlain by down-slope dipping TL torrential/chaotic deposits or by loess, depending on the depth of the erosion. These dissimilar sequences/exposures are labelled OR1…OR9. Except OR1/1, the alternations dip to the SSE as opposed to TL's northerly dips (Fig. 49). As expected, the latter's fan-like distribution matches the conical shape of the underlying FL fan. With OR7 structurally at the base and OR9 at the top, the suite of alternations along the S3 surface/cliff is a key window into the overall OR structure and composition (Figs 47 and 49, Chap.5.4.3).

The OR sequences are described in Chapters 5.4.2.1 to 5.4.2.7 and the origin of OR is discussed in Chapter 5.4.3.

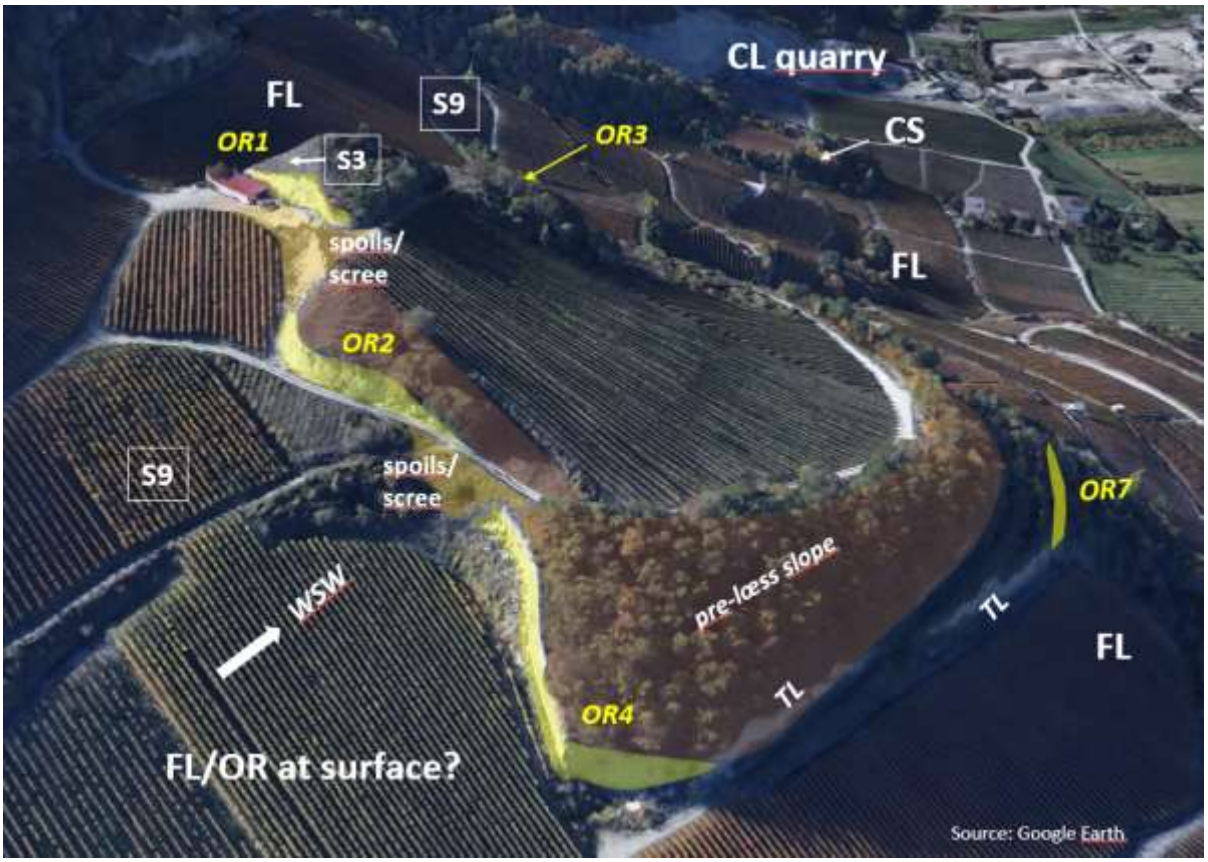

FIGURE 47 Side view of the OR slab resting on the FL fan/S9 surface) and location of its exposures (yellow shaded).

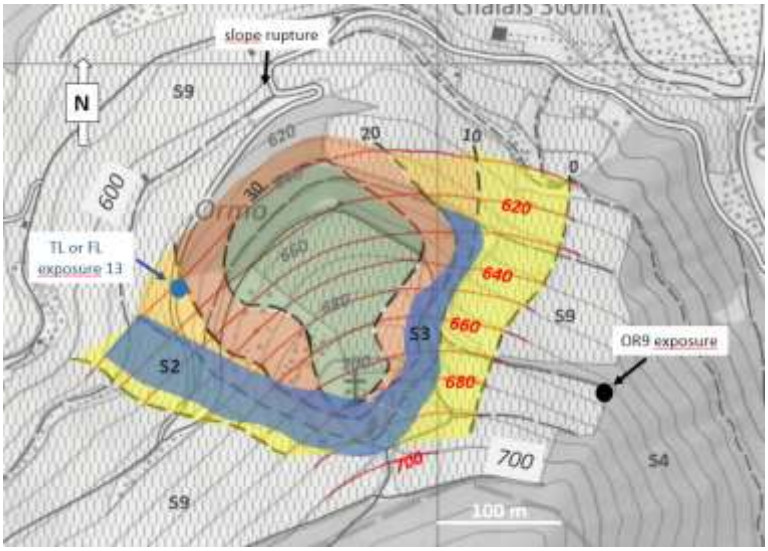

Fig. 48 Approximate isochores (m) of the OR slab between arbitrarily smoothed S9 isohypses (red lines) and the actual surface isohypses (grey lines). The S2 and S3 blue shaded areas are slab boundary cliffs, beyond which the presence of OR at surface is likely.

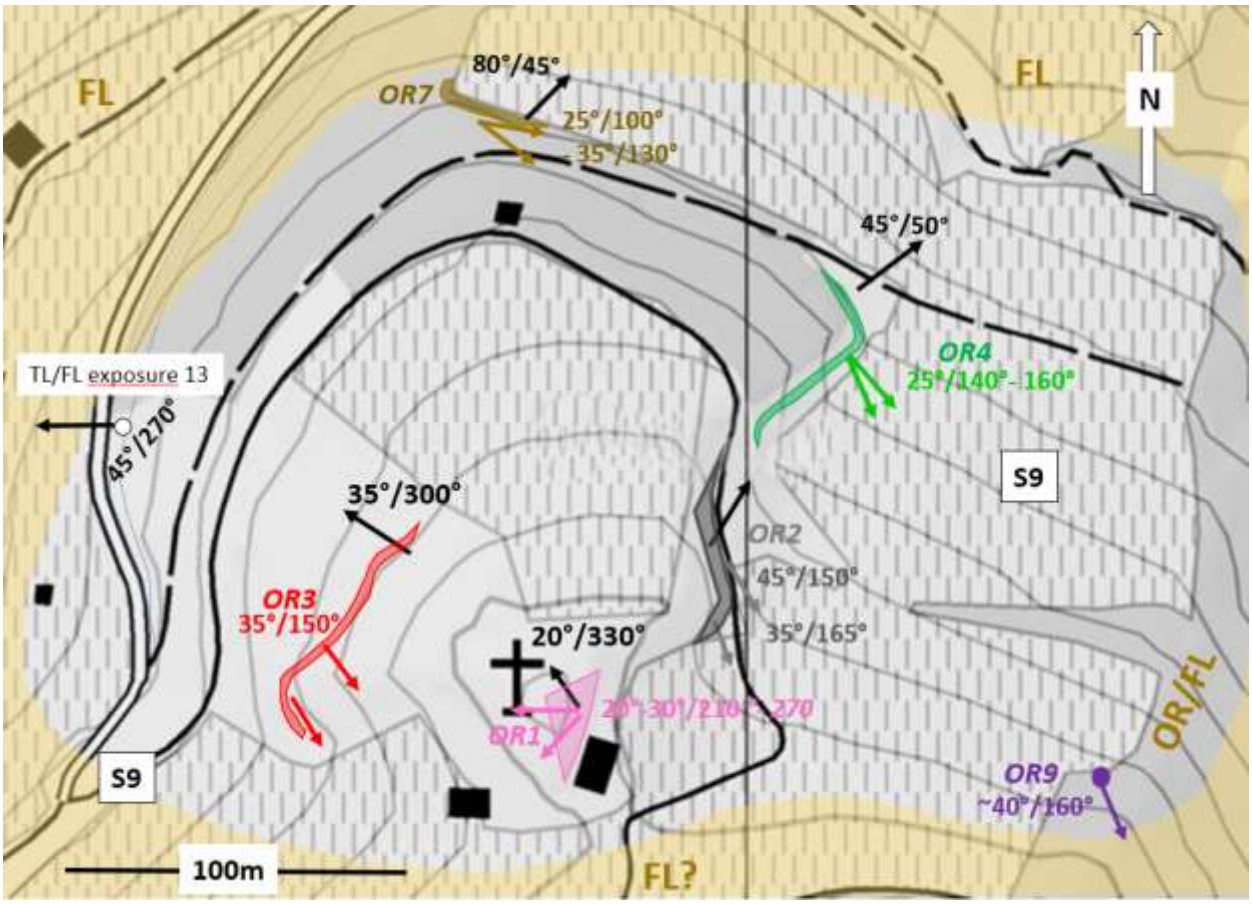

FIGURE 49 Location of the OR exposures showing the dip values and directions of the alternations (coloured arrows) and of those of TL (black arrows). FL and OR slab at surface are respectively yellow and grey shaded.

5.4.2 Sedimentology and petrography

The OR alternations and the deposits of the CL, CS and FL units show common petrographic and sedimentological characteristics (Fig. 50) and therefore share primary sources and depositional processes.

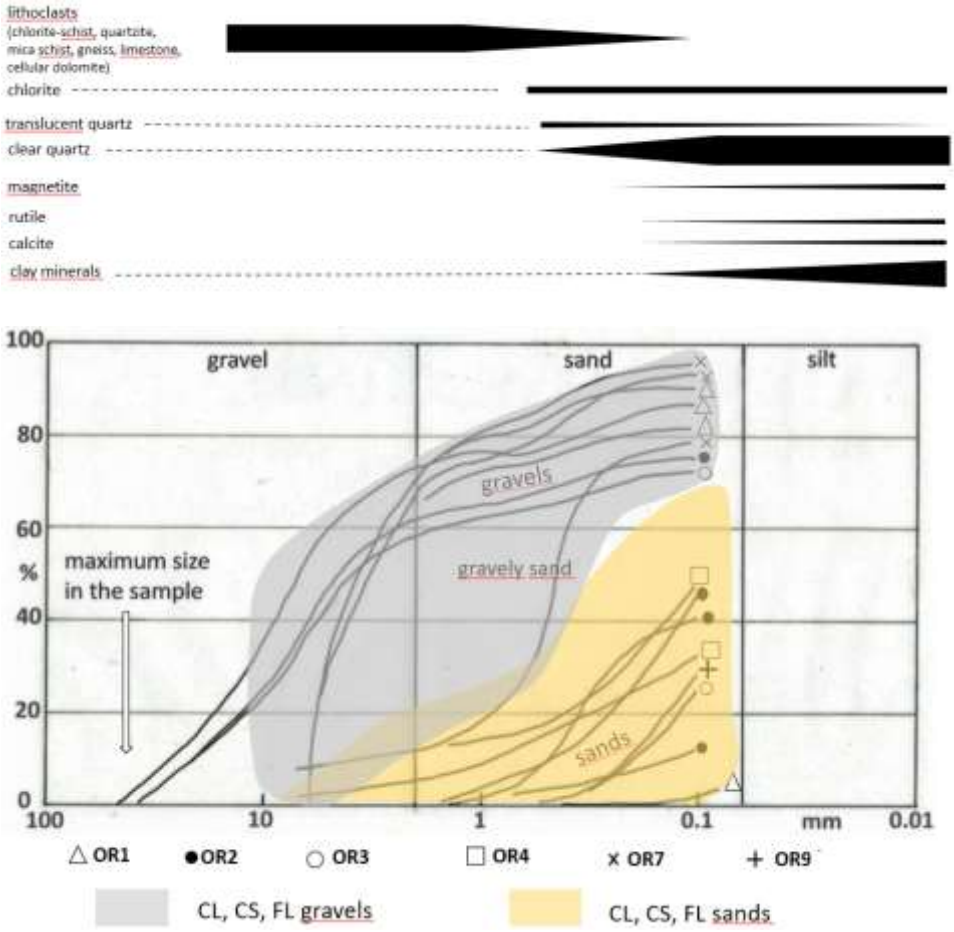

FIGURE 50 Overlap of OR and of CL, CS, FL gravel and sand grading curves. Sample SL 3234 (OR7), a rare gravelly sand, crosses the families' boundaries. The OR1 gravels belong to TL, the other ones to the alternations.

5.4.2.1 OR1 sequence

This sequence consists of the OR1/1 laminated sand overlain by TL (Fig. 51), itself unconformably overlain by pebbly loess.

The beige, 2 m thick **OR1/1** stack of *SFD* includes plant and insect remains (Fig. 53) as well as a decimeter thick interval of convolute varves consisting of dark magnetite-rutile-rich and beige quartz laminae (Fig. 54). The convolution which does not affect the surrounding sand laminae is assumed to be syn-sedimentary. As the OR slab thickness at the OR1 site reaches 20 m minimum (Fig. 48), the OR1/1 thickness most probably exceeds that exposed. A conclusion supported by the past presence of meters thick fine sand a few tens of meters SE of the site (local testimony). The SSW to W directed dips of the sand laminae depart from that of the other alternations (Fig. 49), an apparent anomaly yet to be explained.

TL rests unconformably on an irregular N dipping surface (Figs 51 and 52). It consists of 2 m thick *DFD* (including thin *TD* beds/lenses and one NNW dipping sand bed) overlain by 10 m of chaotic, coarsely stratified *DFD* rich in gneiss, chlorite-schist, etc. cobbles and boulders frequently encrusted by calcite.

FIGURE 51 OR1 exposure. Coarsely stratified, NNW dipping TL overlying the OR1/1 *SFD* stack. The S2 and S3 planar surfaces, from which large boulders emerge, are of pre-loess age.

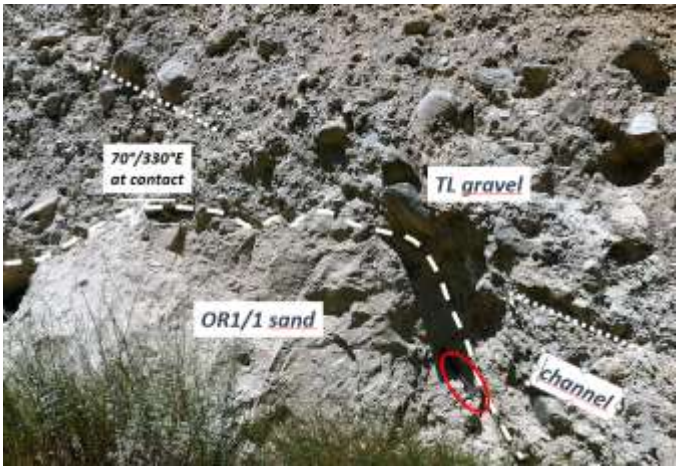

FIGURE 52 Channel within OR1/1 filled by TL. Hammer inside the red lined ellipse.

FIGURE 53 Insect remains (dragonfly wings?) within OR1/1.

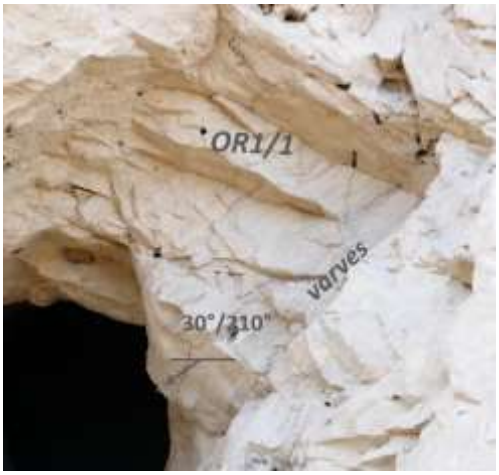

FIGURE 54 Convolute varves within OR1/1.

5.4.2.2 OR2 sequence

The OR2 three-dimensional exposure (Figs 47 and 49) consists of alternating *DFD* and *SFD* layers labelled **OR2/0** to **OR2/7** (Figs 55 to 58), unconformably overlain by a mostly inaccessible thin **TL** of stratified *TD* (Figs 62 and 63), itself overlain by pebbly **loess**. The inclusion of sand chunks within TL (perhaps scraped from OR2/0-3) reminds that observed in FL's TL gravel (Fig. 45).

For reasons not investigated, the general SSE dip of the beds varies from 60°/160°E at the bottom of the alternation to 35°/165°E near its top (Fig. 55), through 40°/160°E and 45°/150°E in the central part (Fig. 49). As suggested by dip disturbances in OR2/0, it is not unlikely that the OR1-OR4 contact may be close to this layer (Fig. 59).

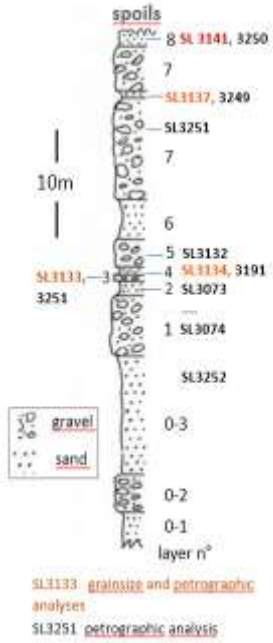

FIGURE 55 Stratigraphy of the OR2 alternation which 45 m thickness along the exposure has been used in the OR emplacement model (Chap. 5.4.3).

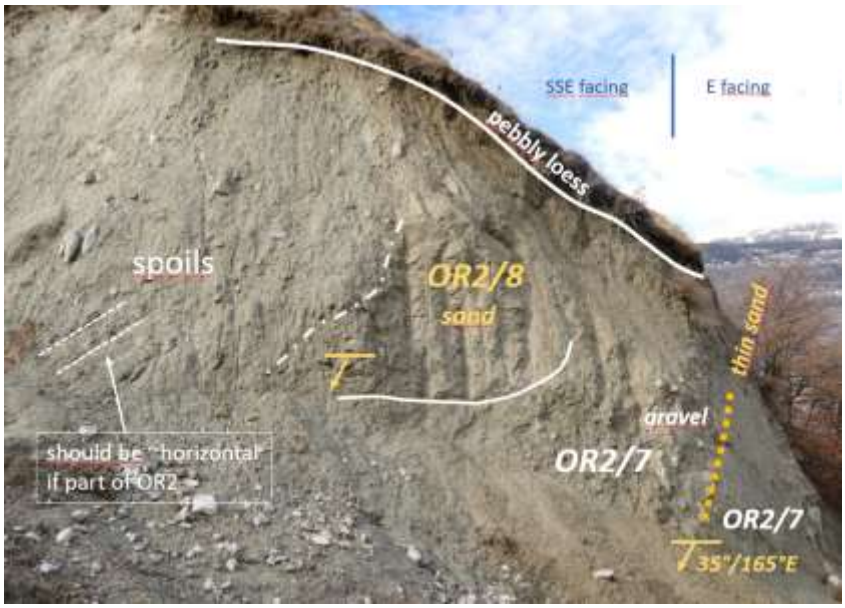

FIGURE 56 Top section of OR2 facing SE (Figs 47 and 49). Due to spoils, the OR2-OR1 relationship is unclear. Downward continuation on Figs 57 and 58.

FIGURE 57 Alternating *DFD* and *SFD* of the E facing OR2 central section. Downward continuation on Fig. 58.

FIGURE 58 E facing bottom section of the OR2 alternation.

FIGURE 59 Anomalous N dipping OR2/0-3 sand laminae.

FIGURE 60 Depositional thickness variation of the OR2/5 *DFD*.

FIGURE 61 Centimeter thick gravel streak parallel to the lamination within the OR2/6 *SFD*.

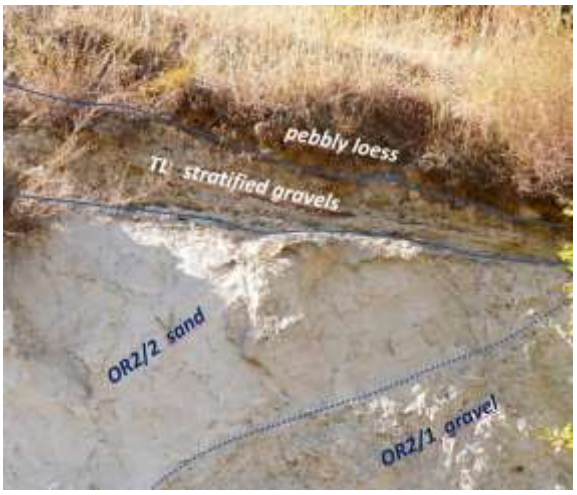

Figure 62 TL stratified *TD* unconformably overlying the OR2 alternation and disconformably overlain by pebbly loess.

Figure 63 *TD* enclosing chunks of fine sand scraped from the surface.

The **alternation's** *DFD* (Fig. 57) generally rest conformably/rarely disconformably on the sand beds, are usually unstratified and show few depositional thickness variations (Fig. 60). Normal grading from multi-

decimeter to centimeter size components occurs in some beds. Gneiss and limestone components are rounded, quartzites angular. As mentioned by Burri (1997), rocks originating from the Zermatt area are also present. The petrographic spectrum (Fig. 50) includes oxidized clasts and plant remains.
The grey beige *SFD* are laminated (Fig. 61). Quartz accounts for 95% of the volume whilst chlorite, magnetite and rutile are concentrated in the remaining 5%.

5.4.2.3 OR3 sequence

This **sequence,** situated on the western side of OR, is exposed along a cliff carved in a landslide detached from the OR slab before **loess** was deposited (Figs 49 and 64). It consists of

- about 10 m thick (base not exposed) SE dipping, alternating *DFD* and *SFD* (**OR3/0** to **OR3/4)** reminiscent of OR2 central section and unconformably overlain by
- a slope-dipping **TL** comprised of *DFD* and a lens of *TD* (Figs. 64 to 66), overlain by pebbly **loess** over the entire length of the exposure.

FIGURE 64 Structure and stratigraphy of the OR3 exposure. The faults (red lines) seem to be related to a landslide (dashed white line), which would explain the variability of the measured dips and dip-directions. The alternation, however, generally dips to the SSE. The PS (light blue) and S2 planar surfaces were generated in pre-loess time.

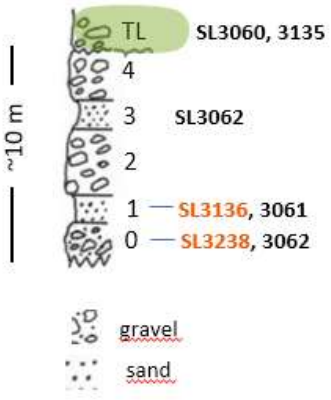

FIGURE 65 OR3 sequence. SL3136 and SL3238 are samples appearing on Fig. 50. Vertical thicknesses along the cliff.

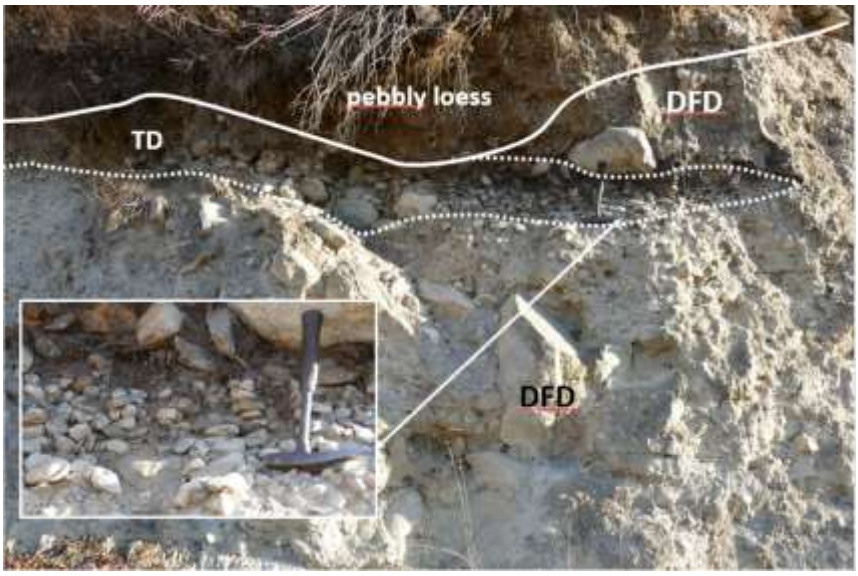

FIGURE 66 Eastern extremity of the OR3 exposure. TL consists of chaotic *DFD* enclosing a lens of *TD*.

5.4.2.4 OR4 sequence

The OR4 exposure consists of a Face A showing most of the alternation and a Face B displaying its basal part, TL and the loess (Figs 49, 67 to 71). As the sub-vertical Face A is nearly parallel to the 50°- 60°E strike of the alternation layers, the latters' traces are close to horizontal.

The **sequence** shows bottom upwards (Fig. 70)

- >10 m (base not exposed) coarsely stratified *DFD* (**OR4/1**) within which the **OR4/2** channel (Fig. 68) has been carved and filled with normally graded coarse to fine *TD* (Figs 69 and 70);
- ~6 m gravelly and laminated *SFD* /*TD* (**OR4/3)** including a 10 cm thick gravel bed;
- ~12 m apparently unstratified, coarse *DFD* (**OR4/4)** containing a few percent of meter-size boulders;
- ~3 m fine *SFD* (**OR4/5**) of which neither the base nor the top is exposed. Its contact with the OR2/0-1 sand is hidden by spoils;
- a chaotic **TL** *DFD*, unconformably overlying OR4/1, but absent above OR4/2, 3, 4 and 5 (Figs 67 to 69 and 71). Its contact with OR4/1 is a smooth surface apparently produced during TL's emplacement (Fig. 72).

TL's exposure continues as a 2 to 10 m high cliff bordering a NNW heading road over a 120 m distance (OR6, Fig. 22). The components of are mostly decimeter size, include meter size boulders and are comprised of quartzite, chlorite- and mica-schists, serpentinite, micro-gabbro and gneiss. Down-slope dipping thin sand layers and frequent calcite encrusting would comfort the attribution of this layer to TL.

A thin pebbly **loess** overlies TL or the alternation.

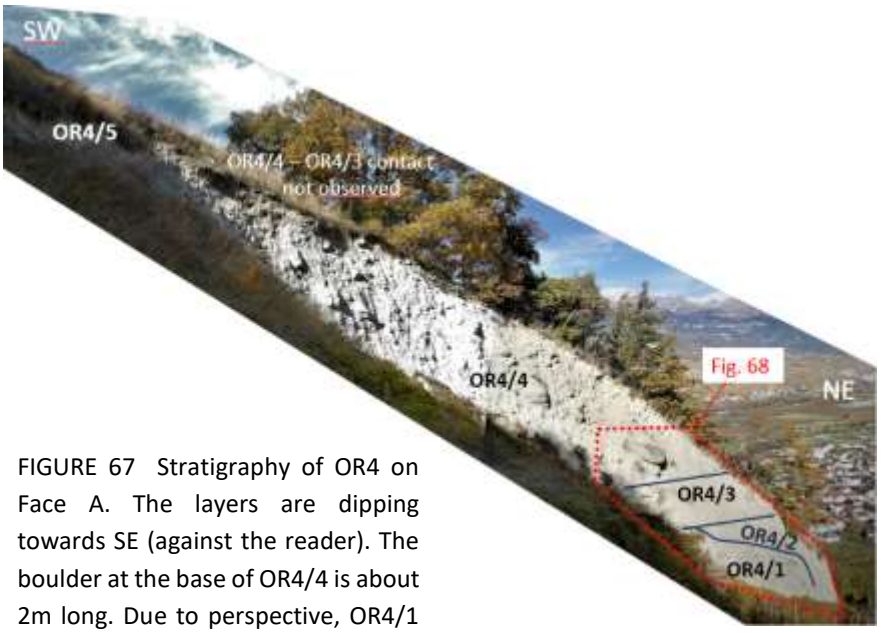

FIGURE 67 Stratigraphy of OR4 on Face A. The layers are dipping towards SE (against the reader). The boulder at the base of OR4/4 is about 2m long. Due to perspective, OR4/1 and OR4/3 appear thinner than they are.

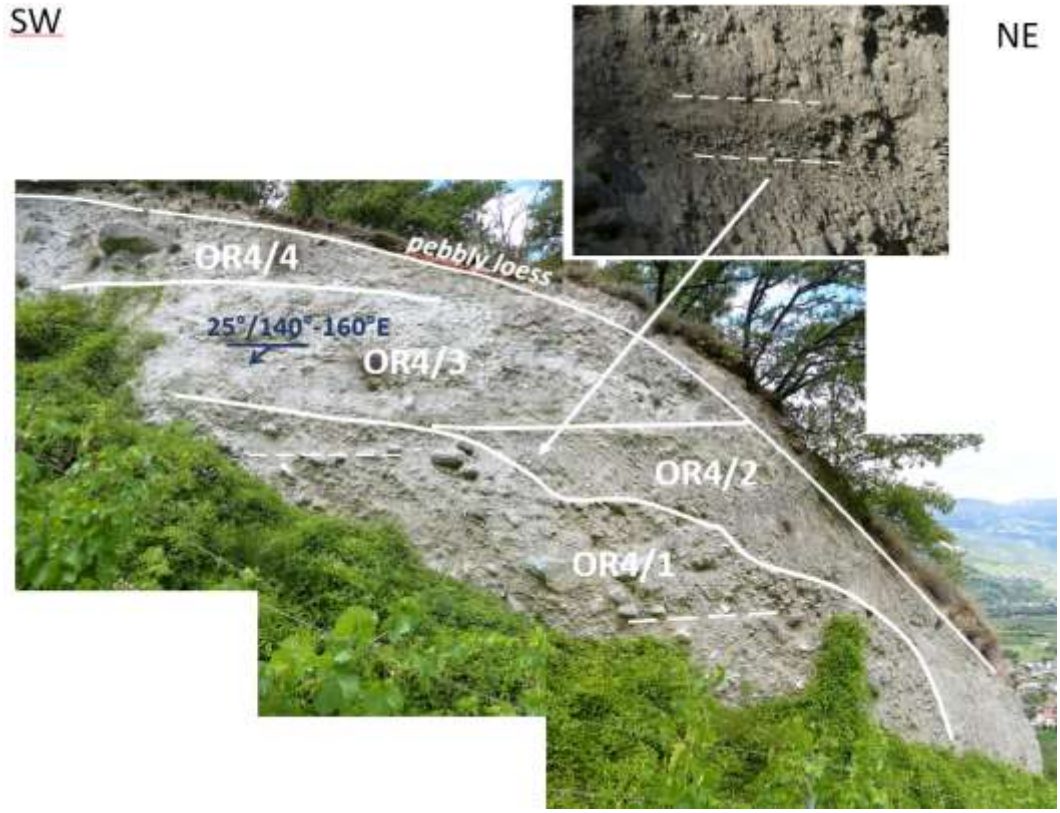

FIGURE 68 Detail of Fig. 67. The channel carved in OR4/1 is filled with OR4/2 gravel. The dip towards 140°E, measured on a sand bed surface, is congruent with the near horizontal traces of the OR4/4-OR4/3 and OR4/3-OR4/2 contacts and with the OR4/1 layering.

FIGURE 69 Normal grading within the OR4/2 channel.

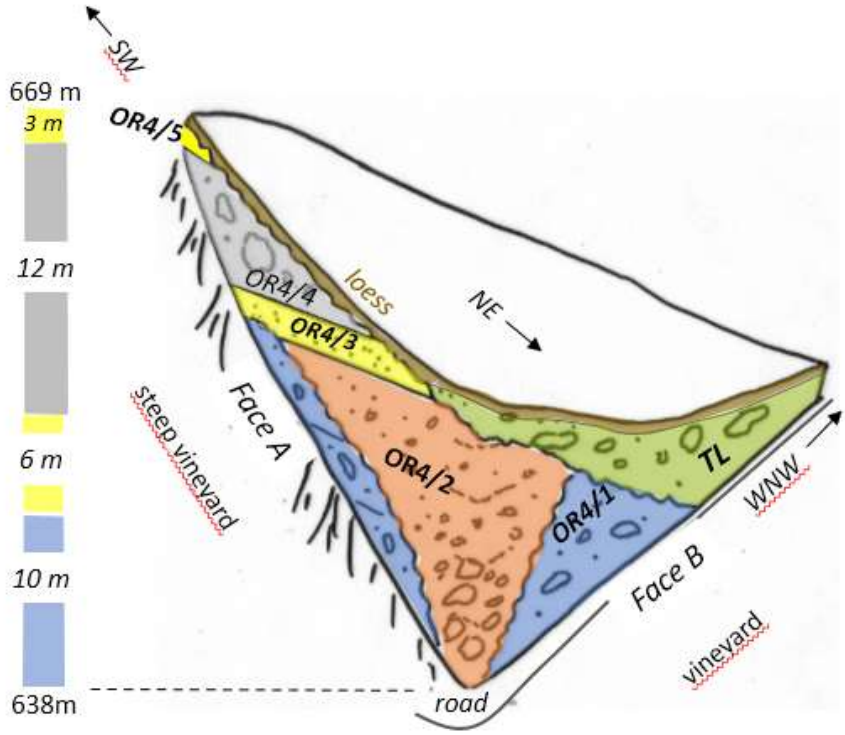

FIGURE 70 On the right, perspective sketch of the OR4 exposure. On the left, stratigraphic column with vertical thicknesses. The OR4/1, 3, 4, 5 layers are dipping to the SSE at ~25°, whilst TL and the loess are dipping to the NE. Thickness-wise the OR4/2 channel is included within OR4/1.

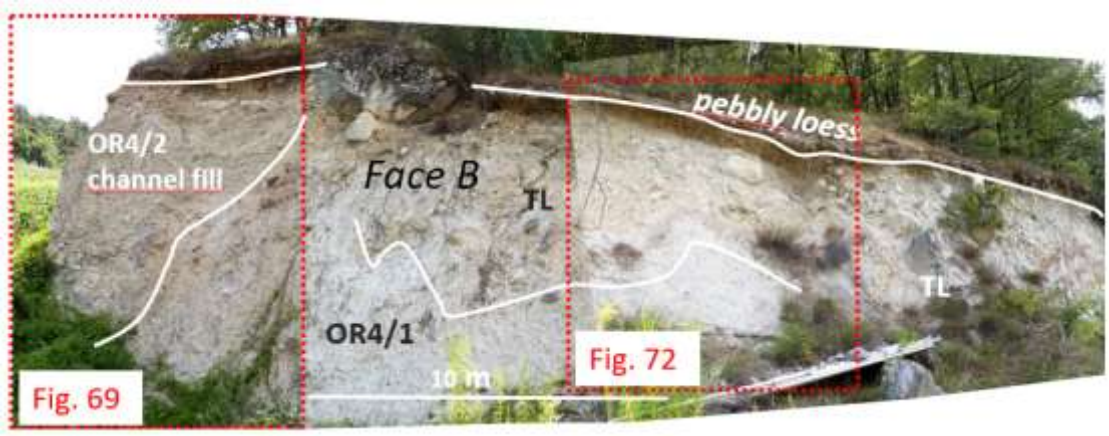

FIGURE 71 OR4/2-OR4/1 and TL-OR4/1 contacts on Face B.

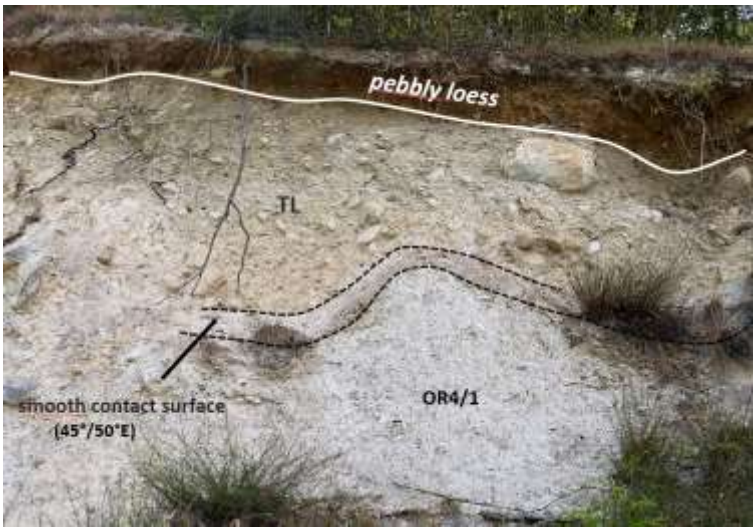

FIGURE 72 Smooth TL-OR4/1 contact surface (face B, Fig. 71). Large boulder about 1.5 m long.

5.4.2.7 OR7 sequence

OR7 is exposed along a 3 to 8 m high and 100 m long cliff broadly parallel to the ESE alternation's dip direction (Figs 47 and 49). The short **alternation**, visible at the western extremity of the exposure, is comprised of 2 m unstratified *DFD* (**OR7/1**, base not exposed) conformably overlain by 4 m of laminated *SFD (***OR7/2**) (Figs 73 and 74). The latter's basal 1.5 m are fine (OR7/2a) and the overlying 2.5 m gravelly (OR7/2b). The NE dipping **TL** occupies the remaining exposure length. Its contact with OR7/2 is a smooth surface (Fig. 75).

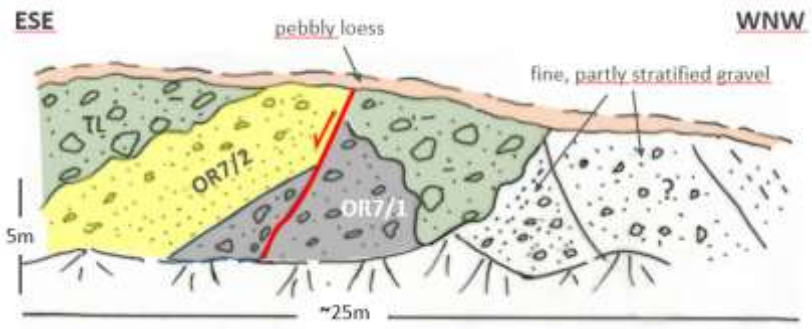

FIGURE 73 Sketch of the OR7 exposure. The relation of the westernmost gravels to the alternation could not be unravelled.

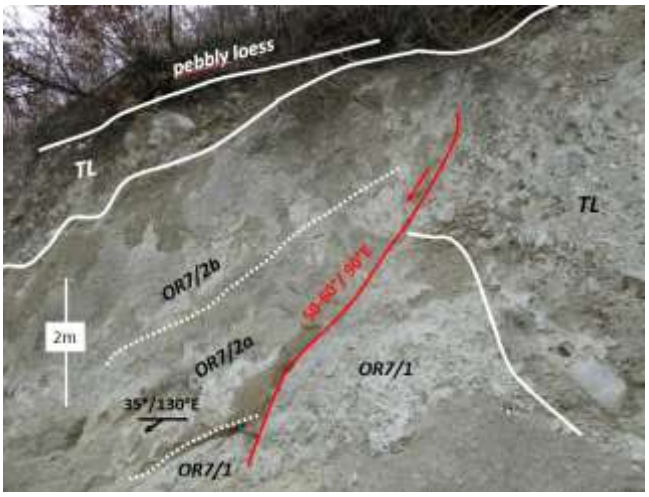

FIGURE 74 OR7 sequence. The superficial fault cutting OR7 post-dates TL and pre-dates the loess deposition.

FIGURE 75 Smooth TL-OR7/2 contact surface.

5.4.3 Origin of the Ormeaux slab

Near the top of the Ormeaux hill, Burri (1997) mentions counter slope-dipping sand and coarse gravel layers comprised of gneiss, quartzite and rocks of the Zermatt area and relates these deposits to the proximity of the RG. In the wake of this report the Ormeaux slab appears as "Moraine de la dernière glaciation" on SGA sheet 111 (Gabus et al. lit. cit.), which is considered incompatible with the facts. A new interpretation is thus required which should explain

1. the juxtaposition, along the slope, of dissimilar *DFD-SFD* alternations unconformably overlain by the ubiquitous down-slope dipping TL;
2. a 290 m long suite of reversed dips (Figs 49 and 76);
3. the general absence of structural disturbances within the alternations except at their extremities (as observed in OR2 and assumed for the other alternations);
4. the lithological/mineralogical composition and texture of all the *DFD*, *SFD* and *TD* being identical to those of the underlying FL fan;
5. the stratigraphic dissimilarity of the alternations.

The simple, alternative proposed 2D model, which is based on data (thicknesses, lengths) of the short but uninterrupted OR2-OR4 suite, ought to apply to the entire OR slab since lithologies and general dip direction are shared by all the alternations and ought to broadly satisfy the above requirements. In this model, *the counter-slope dips result from detached FL slices sequentially sliding and reversing their dip direction as they first override FL's surface and subsequently enter in contact with the preceding slice* (Fig. 76). Such rotational slides are well documented (Dikau lit.cit.; Buma et al. 1996).

Regarding point 2, a split in individual slices is required to relate the total length of the alternations' suite to the thickness of the original slice (or depth of the decollement/sole), as the length of an alternation along the slope should slightly exceed the thickness of the original slice. This obviously cannot be the case for a single 290 m long slice. In the OR2 case, the 45 m long suite of reversed dips (spoils excluded) requires a ~45 m thick slice thickness (Fig. 55), which is not exceptionally large (Booth at al., 2013). This figure, which exceeds the 30 m plus shown on Figure 48, infers that the sole of OR is deeper than FL's smoothed surface (as to be expected).

Regarding point 5, it is assumed that the lateral offsetting of OR2 and OR4 may explain their stratigraphic differences. The stratigraphic differences among the other short, poorly exposed alternations are expected in such a terrestrial environment and of little concern.

An alternative explanation deriving the alternations from the collapse, along lystric faults, of kame terraces would require longer displacements, internal disturbances and a higher similarity of the alternations, and would explain neither the overwhelming presence of *DFD* and *SFD* nor the large volume of the slab.

In brief, *the OR slab is interpreted as a large landslide composed of slices overriding each other, partly levelled by erosion and unconformbly overlain by TL*. The uncertainties attached to this model preclude any detailed kinematics being proposed.

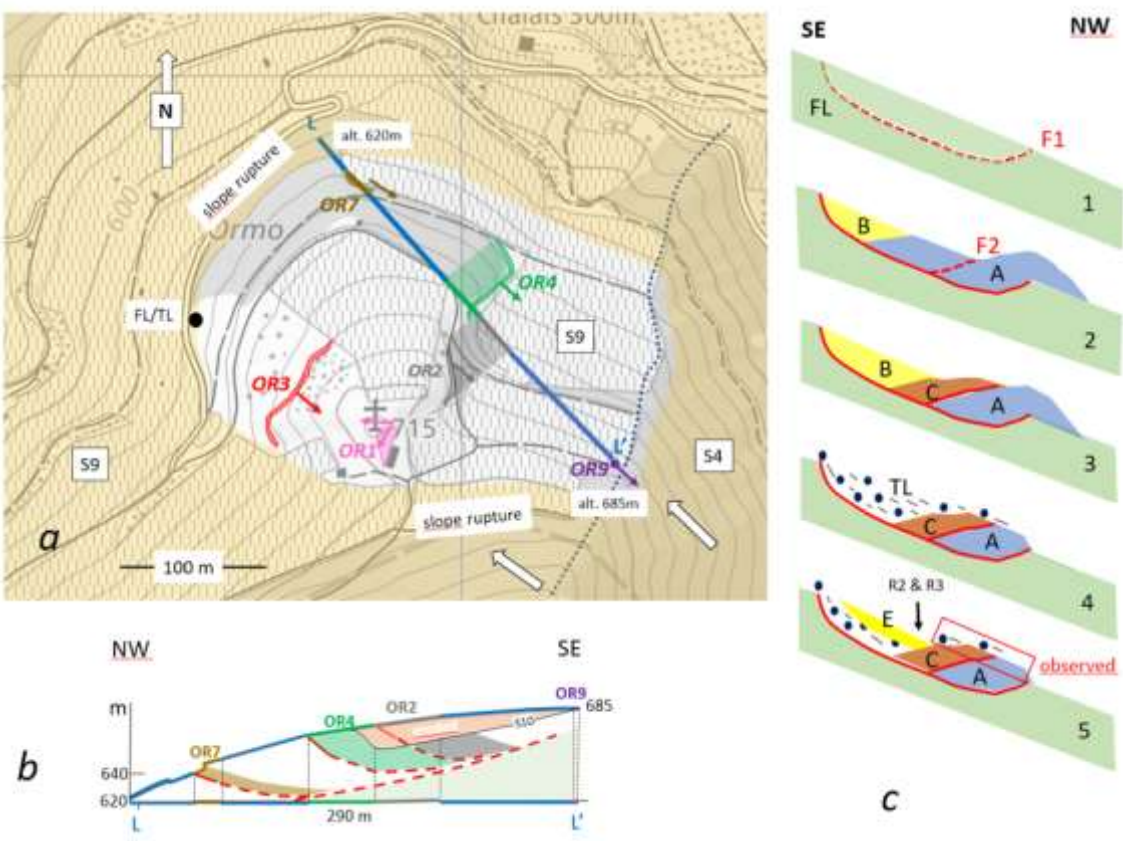

FIGURE 76 Proposed OR emplacemen model . *a* Trace L-L' of the geological cross-section. The blue stretches along the surface line represent exposure gaps. The white arrows show the sliding direction of the alternations (i.e. parallel to the dip directions); *b* Hypothetical cross-section of OR along the LL' trace; *c* OR emplacement model whereby

1. sliding surface F1 develops within FL;
2. slice A slides and partly overrides FL which generates counter-slope dips and open space B. F2 surface develops;
3. slice C comes in contact with slice A and open space B increases;
4. A and C are partly levelled and covered by TL, following the filling of the B depression;

5.5 South flank: discussion and conclusions

Deposits

The structural and sedimentological characteristics of the matrix-supported gravels within the CL1, CS1, FL1 members and within OR are well known from *DFD,* as discussed in Chap 4.6. The associated subordinate clast-supported gravels, characterized by rounded/subrounded components, are interpreted as *TD* (Recking et al. lit. cit.; Beauchamp lit. cit.). The CL2, CS2, FL2 fine laminated sands, as well as those intervening within FL1 and OR, are interpreted as *SFD* (Sohn et al. lit. cit.) emplaced as thin slurries. The mechanisms leading to the alternation of *DFD*, *SFD* and *TD* have yet to be identified.

TL's ubiquitous chaotic TLa base is characterized by lack of or faint stratification, higher content of moraine material such as striated serpentinite, very large gneiss and chlorite-schist boulders and frequent calcite encrusting. Whether it represents Debris Avalanche or Rock Flow deposits*,* etc*.* (Dikau et al. 1996; Coussot et al. lit.cit.; Hungr et al. 2001, Reznichenko et. al. 2012) is open to discussion. The occasionally enormous boulders scattered in the fans' original area are attributed to TLa. The overlying stratified TLb, deposited/preserved on the FL fan only, is assumed to represent late fluxes of *DFD* and *TD.*

Environment of deposition

The **FL** body, including the **OR** landslide, shows characteristic alluvial fan features such as conical shape, down-dip thickness increase and association of *DFD*, *SFD* and subordinate *TD*. Partly eroded **CL** and **CS** show fan sedimentological characteristics as well (Figs 20a, 22 and 24). The varying dip directions of CL's *DFD* (Figs 30 and 31) suggest a lobate architecture which could not be demonstrated elsewhere.

Lateral and longitudinal extensions

The original area of the CL, CS and FL fan complex extended from close to CL's western erosional flank to a few hundred meters E of the RR gorge. These fans certainly contributed to the filling of the RV and were emplaced before the Sierre landslide, a hypothesis that seismic data could test.

The OR landslide original size certainly exceeded that of the current slab as suggested by its erosional flanks and by the existence of an isolated exposure on FL's S9 surface.

Sources and climate

The lithological spectrum common to all those deposits indicates that formations of the SM nappe were the primary source of much of the fans' material. As on the opposite side of the RV, the melting of rock glacier(s) (secondary source), and abundant precipitations presumably led to the release of large amounts of *DFD.* These rock glaciers were most probably located within the Réchy glacial valley (before its torrential deepening) the flanks of which mainly consist of SM nappe formations (Figs 19 a and b). Contributions from the Le Tsan glacial cirque, however, cannot be excluded.

The meters thick *SFD* member and the intervening *SFD* layers require a source/ water expanses from which thin sand slurries could rhythmically escape (mechanism?). It is assumed that the proximity of the *SFD* and *DFD* sources would best explain their alternation. On the other hand, the abrupt transition from CL1, CS1, FL1 to CL2, CS2, FL2 and eventually to TL had to be linked to the near/total exhaustion of the *DFD* secondary source.

The source of the chaotic and ubiquitous TLa layer is less obvious, especially with respect to its occasionally enormous boulders. Those probably originated from moraines deposited on the slopes by the VR and Rhône glaciers, as were the equally large boulders encountered within CL1, CS1 and FL1. The source of the TLb deposits could involve both moraine and residual rock glacier.

Above about ~1000 m, the *SD* transport followed the SSE-NNW trending VR, at an angle to the S-N trending RR gorge which later incised the FL fan and the Carboniferous substratum. The reason of this trend change is not known.

Fans' age

The sequence of events extending from the emplacement to the partial erosion of the fans is the same on both sides of the RV and thus taken as regionally representative. For want of hard data, it is assumed that the *DFD*, *SFD* and *TD* were generated during the Late Glacial to Early Holocene period of instability that has been identified in the Alps (Dapples 2002; Le Roy 2012) and particularly in eastern Valais (Moulin 2014). Obviously, dating (OSL, C_{14}) of the *DFD*, *SFD* and loess would vastly improve this analogical approach.

Sequence of events (Fig. 78)

1 carving of the RV flank by the RG and of the VR (down to 1000 m?) by the eponymous glacier and deposition of moraines;
2 building of the FL, CS and CL fans (excluding TL);
3 emplacement of the OR landslide;
4 erosion followed by deposition of TL, unconformably on OR and disconformably elsewhere;
5 carving of surfaces S1, S2 and S3 by torrents R1, R2 and R3;
6 carving of the RR gorge (R4) and synchronous building of the Réchy fan and deepening of the VR glaciated valley;
7 loess deposition;
8 limited erosion and anthropic interventions.

The partial filling of the RV by the CL, CS and FL fans ended with step 4. The data at hand do not allow to determine whether the Sierre landslide was emplaced after step 4 or after step 6.

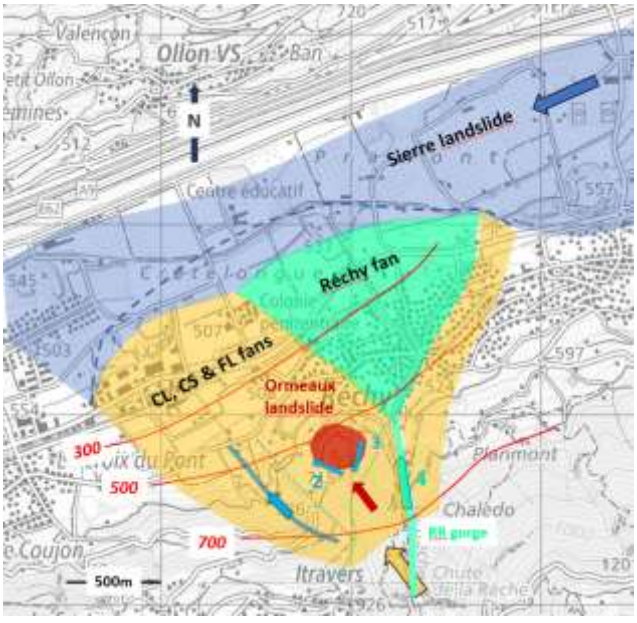

Fig. 78 Map view of events 2, 3 and 6. Alluvial fans developed over the yellow shaded area part of which was overlain by the Réchy fan (light blue green). The dashed blue represents a hypothetical maximum extension of the fans. The direction of the *SD* (yellow arrow), of ravine 1 (blue arrow) and of the OR landslide (red arrow) is the same as that of the VR (Fig. 19b). The RR gorge (green arrow) incises the FL fan at an angle with the top substratum isohypses (continuous red lines, meters a. m. s. l.). E of the RR gorge and above 700 m, FL has been eroded - it was presumably thin - by the RR (R4).

6 Conclusion: the central Rhône valley and its flanks

As the main conclusion of this work, it can be stated that the bodies of Quaternary deposits resting on the flanks of the central RV and described as Rhône or Last Glaciation moraines on SGA sheets 35 and 111 are in fact Late Glacial to Early Holocene* alluvial fans or their remnants. These are built of debris-flow, subordinate sand-flow (S flank only) and torrential deposits issued from rock glaciers and water expanses storing scree and sand. RG and local moraine material scattered on the slopes was also included in the debris-flows and became abundant in the top chaotic deposits as the main sources became exhausted. The fans of the S flank contributed to the filling of the RV and were likely emplaced before the famous Sierre landslide*. It is assumed that the mobilization of the sources was triggered by permafrost melting and abundant precipitations resulting from atmospheric warming that the very nature of deposits, the presence of weathered boulders, reddened clasts and remains of insects, molluscs and plants, and the general slope instability attest. The latter is best expressed by the large, so far unrecognized Ormeaux landslide detached from and lying on the largest fan of the RV South flank.

A totally new Quaternary story has thus emerged, which started with the building alluvial fans, continued with their partial erosion and essentially ended with the deposition of the loess. This period of erosion was demonstrably also responsible for the carving of the RR gorge and the synchronous building of the Réchy fan on the S flank.

Whether the complexes of fans deserve Formation status could perhaps be envisaged.

*Hypothesis

Declarations

Ethics approval and consent to participate: not applicable.

Consent for publication: not applicable.

Availability of data and materials: the samples were not stored, but equivalents can be collected at outcrops mentioned the text. Nevertheless, organic remains (plants, wood, insects, molluscs) as well as samples for C_{14} and OSL are still available from the author.

Competing interests: not applicable.

Funding: not applicable.

Author's contributions: not applicable.

Acknowledgements: the author is indebted to his friends Filippo Bianconi and late Walter Ziegler for early discussion of this work.

Author's information: totally independent work

References

Amelot, F., Delannoy, J.-J. & Nicoud, G. (2003) L'édification des cônes de déjection en montagne : intérêts paléeoenvironnemental et hydrologique, contribution typologique. *Quaternaire 14 (4), 253-263.*

Badoux, H., Bonnard, E.G., Burri, M. & Visher A. (1959). Levé géologique. Feuille 35 St-Léonard. *Atlas géol. Suisse 1 :25 000*

Badoux, H., Bonnard, E.G., & Burri, M. (1959). Notice explicative. Feuille 35 St-Léonard. *Atlas géol. Suisse 1 :25 000*

Bardou, E. & Jaboyedoff, M. (2008) Debris flows as a factor of hillslope evolution controlled by a continuous or a pulse process. *Geological Society, London, Special Publications, 296, 63-78.*

Beauchamp, J. (2020) Sédimentologie. *www.u-picardie.fr*

Besson, O., Rouiller, J.D., Frei, W. & Masson, H. (1993). Campagne de sismique-réflexion dans la vallée du Rhône entre Sion et St-Maurice : perspectives d'exploitation géothermique des dépôts torrentiels sous-glaciaires. *Bull. Centre hydrol. et géotherm. (CHYN).* 12*:* 45-63.

Bini, A., Buoncristiani, J.F., Couterrand, S., Ellwanger, D., Felber, M., Florineth, D., Graf, H.R., Keller, O., Kelly M., Schlüchter, C. & Schoeneich, P. (2011). Switzerland during the Last Glacial Maximum. *Federal Office of Topography swisstopo, CH-3084 Wabern, Switzerland.*

Booth, A.M., Lamb, M.P., Avouac, J.-Ph., Delacourt, CH. (2013) Landslide velocity, thickness, and rheology from remote sensing: La Clapière landslide, France. *Geophysical Research Letters/Volume 40, Issue 16.*

Buma, J. & Van Asch, T. (1996). Slide (rotational). In: *Landslide Recognition, Identification, Movement and Causes. Edited by R.Dikau, D. Brundsen, L. Schrott & M.L. Ibsen. Wiley.* 251 pp*.*

Burri, M. (1955). La géologie du Quaternaire aux environs de Sierre. *Bull. Soc. Vaud. Sc. Nat.* 66/289 : 141-154.

- (1958). La zone de Sion – Courmayeur au Nord du Rhône. *Matériaux Carte Géol. Suisse, Nouvelle Série, 105^{e} livraison.*
- (1997). Géologie récente de Finges et de ses environs (VS). *Bull. Murith*. 115 : 5-27.

Canton du Valais (2007). Etudes des terroirs (Etude Sigales). *https://www.vs.ch>web>etude-des-terroirs.*
INTERPROFESSION DE LA VIGNE ET DU VIN DU VALAIS (2004). Etude géopédologique des vignobles de St-Léonard-Flanthey. *www.lesvinsduvalais.ch*

Christ, P. (1925) Die Walliser Anthrazilagerstätten und der Walliser Anthrazitbergbau während der Jahre 1917-1924*. Beitr. Geol. Schweiz*. Ser. 11/2 : 1-162.

Chambon, G. & Laigle D. (2013). Les laves torrentielles. In : *Torrents et rivières de montagne. Dynamique et aménagements. Versailles : Quae, 200-266.*

Cojan, I. & Renard, M. (2006). *Sédimentologie.* Dunod, Paris. 444 pp.

Corominas, J., Remondo, J., Farias, P., Diaz de Teran, J., Dikau, R., Schrott, L., Moya, J. & Gonzalez, A. (1996). Debris flow. In: *Landslide Recognition, Identification, Movement and Causes. Wiley.* 251 pp*.*

Coussot, P. & Meunier, M. (1996). Recognition, classification and mechanical description of debris flows. Earth-Sci. Rev. 40, 209-227.

DAPPLES, FL. (2002) Instabilités de terrain dans les Préalpes fribourgeoises (Suisse) au cours du Tardiglaciaire et de l'Holocène : influence des changements climatiques, des fluctuations de la végétation et de l'activité humaine. Geofocus 6, Fribourg 2002.

Dikau, R. (Editor), Brunsden, D. (Editor), Schrott, L., (Editor), Ibsen, M.L. (1996). Landslide Recognition. Identification, Movement and Causes. Wiley, 251 pp.

Dorthe-Monachon, L. 1993. Etudes des stades tardiglaciaires des vallées de la rive droite du Rhône entre Loèche et Martigny. *Travaux Inst. Géogr. Lausanne* 190 : 1-142.

Gabus, J.-H., Weidmann, Sartori, M., Burri, M. (2008a). Notice explicative. Feuille 1287 Sierre. *Atlas géol. Suisse 1 :25 000.*

Gabus, J.-H., Weidmann, M., Bugnon, P.C., Burri, M., Sartori, M. & Marthaler, M. (2008b). Levé géologique. Feuille 1287 Sierre. *Atlas géol. Suisse 1 :25 000*

Guelat, M. (2013). Le loess de la vallée du Rhône. Présentation lors de « Les Alpes valaisannes Terre de rêve des géologues ». Sion, 7 et 8 novembre 2013.

Highland, L.M. & BOBROWSKI, P. (2008). The Landscape Handbook – A guide to understanding landslides. *https//: pubs. usgs. gov/circ/1325/pdf/Sections/Section1.pdf.*

Hungr, O., Evans, S.G., Bovis, M.J. & Hutchinson, J.N. (2001). A Review of the Classification of Landslides of the Flow Type. *Environmental & Engineering Geoscience, Vol VII, N°.3, 221-238.*

LE ROY, M. (2012) Reconstitution des fluctuations glaciaires holocènes dans les Alpes occidentales – Apports de la dendrochronologie et des datations par isotopes cosmogéniques produits in situ. *Thèse Université de Grenoble, 2012.*

LELEU, S. (2005.) Les cônes alluviaux, Crétacé Supérieur/ Paléocène en Provence : traceurs de l'évolution morpho-tectonique des stades précoces de collision. *Doctoral Thesis, Louis Pasteur University, Strasbourg.*
Marthaler, M., Sartori, M., Escher, A. & Meisser, N. (2008). Atlas Geologique de la Suisse 1 :25'000, Feuille 1307 Vissoie. Notice explicative. *Office fédéral de topographie swisstopo.*

Marthaler, M., Sartori, M., Escher, A. (2008). Atlas Geologique de la Suisse 1 :25'000, Feuille 1307 Vissoie. Levé géologique. *Office fédéral de topographie swisstopo.*

Massaad, M. (1973) pétrographie de quelques shales de l'Aalénien de l'Helvétique et de l'Ultrahelvétique. Bull.Lab. Géol. Minéral. Géophys. Musée géol. Univ. Lausanne 203.

Moulin, B. (2014). L'habitat alpin de Gamsen (Valais, Suisse). 2. Le contexte géologique. Histoire sédimentaire d'un piémont en contexte intra-alpin, du tardiglaciaire à l'actuel. Avec Contribution de Michel Guélat et Philippe Rentzel. *Cahiers d'archéologie romande* 154. *Archaeologia Vallesiana* 12.

Nemec, W. & Steel, R.J. (1984). Alluvial and coastal conglomerates: their significant features and some comments on gravely mass-flow deposits. In: Koster, E.H. & Steel, R.J. (Eds) Sedimentology of Gravels and Conglomerates. *Canad. Soc. Petrol. Geol., Mem. 10, 1-31.*

Novak, A., Tomislav, P. & Smuc, A. (2018) Sedimentological and geomorphological characteristics of Quaternary deposits in the Planica-Tamar Valley in the Julian Alps (NW Slovenia). *Journal of Maps, 14:2, 382-391.*

Recking, A., Richard, D. & Degoutte, G. (2013) Torrents et rivières de montagne. Dynamique et aménagement. *Editions QUAE*.

Rosselli, A. & Olivier, R. (2003). Modélisation gravimétrique 2.5D et cartes des isohypses au 1 :100'00 du substratum rocheux de la Vallée du Rhône entre Villeneuve et Brig (Suisse*). Eclogae geol. Helv. 96*, 399-423.

Scapozza, CR. (2012) Stratigraphie, morphodynamique, paléoenvironnements des terrains sédimentaires meubles à forte déclivité du domaine périglaciaire alpin. *Institut de géographie, Université de Lausanne, Anthropole, 1015 Lausanne.*

Silhan, K. & Panek, T. (2010) Fossil and recent debris flows in medium-high mountains (Moravskoslezské Beskydy Mts, Czech Republic). *Geomorphology, vol. 124, iss. 3-4, 238-249.*

Schaechtlin, Ph. (2000a). Etude gravimétrique de l'éboulement de Sierre. *Travail de diplôme, Sciences de la Terre, Université de Lausanne, non publié.*

Schaechtlin, Ph. (2000b). Etude du quaternaire de l'éboulement de Sierre. *Travail de diplôme, Sciences de la Terre, Université de Lausanne, non publié.*

Scholle, P.A. (1979). A Color Illustrated Guide to Constituents, Textures, Cements and Porosities of Sandstones and Associated Rocks. *Memoir 28, published by The American Association of Petroleum Geologists, Tulsa, Oklahoma, U.S.A.*

Sohn Young Kwan, Chul Woo Rhee & Bok Chul Kim (1999). Debris Flow and Hyperconcentrated Flood-Flow Deposits in an Alluvial Fan, Nortwest Part of the Cretaceous Yongdong Basin, Central Korea. The Jrnl of Geology, 107: 111-132.

Steck, A., Allimann, M., Epard, J.L., Escher, A., Gouffon, Y., Lempika Münch, A., Marthaler, M., Masson, H., Mosar, J., Sartori, M. & Spring,L. (1999). Carte tectonique des Alpes de Suisse occidentale et des régions avoisinantes. Carte géologique spéciale N° 123-NW. Feuille 41 Col du Pillon

Tricart, J. (1965). *Principes et méthodes de géomorphologie*. Masson, Paris, 496 pp.

Winistoerfer, J. (1978). Paléogéographie des stades glaciaires des vallées de la rive gauche du Rhône entre Viège et Aproz. *Bull. Murith*. 94 (1977): 1-65.